Spring 2004

Timing and Paleoclimatic Significance of Latest Pleistocene and Holocene Cirque Glaciation in the Enchantment Lakes Basin, North Cascades, WA

Eric L. (Eric Leland) Bilderback
Western Washington University

TIMING AND PALEOCLIMATIC SIGNIFICANCE OF LATEST PLEISTOCENE AND HOLOCENE CIRQUE GLACIATION IN THE ENCHANTMENT LAKES BASIN, NORTH CASCADES, WA

BY

ERIC L. BILDERBACK

Accepted in Partial Completion

of the Requirements for the Degree

Master of Science

Moheb A. Ghali, Dean of the Graduate School

ADVISORY COMMITTEE

Chair, Dr. Douglas H. Clark

Dr. Bernard A. Housen

Dr. Christopher A. Suczek

MASTER'S THESIS

In presenting this thesis/field project in partial fulfillment of the requirements for a master's degree at Western Washington University, I agree that the Library shall make its copies freely available for inspection. I further agree that copying of this thesis/field project in whole or in part is allowable only for scholarly purposes. It is understood, however, that any copying or publication of this thesis/field project for commercial purposes, or for financial gain, shall not be allowed without my written permission.

Signature _____

Date May, 14 2004

MASTER'S THESIS

In presenting this thesis in partial fulfillment of the requirements for a master's degree at Western Washington University, I grant to Western Washington University the non-exclusive royalty-free right to archive, reproduce, distribute, and display the thesis in any and all forms, including electronic format, via any digital library mechanisms maintained by WWU.

I represent and warrant this is my original work and does not infringe or violate any rights of others. I warrant that I have obtained written permissions from the owner of any third party copyrighted material included in these files.

I acknowledge that I retain ownership rights to the copyright of this work, including but not limited to the right to use all or part of this work in future works, such as articles or books.

Library users are granted permission for individual, research and non-commercial reproduction of this work for educational purposes only. Any further digital posting of this document requires specific permission from the author.

Any copying or publication of this thesis for commercial purposes, or for financial gain, is not allowed without my written permission.

Name: Eric L. Bilderback

Signature: _

Date: 20 June 2018

TIMING AND PALEOCLIMATIC SIGNIFICANCE OF LATEST PLEISTOCENE AND HOLOCENE CIRQUE GLACIATION IN THE ENCHANTMENT LAKES BASIN, NORTH CASCADES, WA

A Thesis
Presented to
the Faculty of
Western Washington University

In Partial Fulfillment
of the Requirements for the Degree
Master of Science

by
Eric L. Bilderback
May 2004

Abstract

The Enchantment Lakes Basin in the Alpine Lakes Wilderness, Washington, preserves two sets of moraines that record distinct post-Wisconsin maximum advances of cirque glaciers in the eastern North Cascades. Cores collected from five lakes adjacent to the moraines indicate that there were two Neoglacial advances, culminating with the Little Ice Age, and one slightly larger advance that ended coincident with the termination of the North Atlantic Younger Dryas event. The cores show no evidence for an early Holocene advance, in contrast to some other studies in the North Cascades. (e.g., Heine,1998; Thomas, 1997; Thomas et al., 2000).

Upstream glacier activity, as indicated by rock-flour production, is recorded in the lake sediments as fluctuations in magnetic susceptibility, organic content, and sediment particle size. Tephra identification, AMS ^{14}C dating, and paleomagnetic secular variation of the sediments provide detailed age constraints for the lake cores. The presence of the 475 cal yr B.P. Mount St. Helens W_n tephra within outwash associated with the inner (Brynhild) moraines indicates that they are Little Ice Age (LIA) equivalent. The age constraints on the lake sediments show that this advance began between ~1000-800 cal yr B.P. and culminated after the W_n tephra was deposited. The age of the outer (Brisingamen) moraines, previously reported as early Holocene (Waitt et al.,1982), are instead latest Pleistocene; close limiting ^{14}C dates demonstrate that this advance ended shortly before ~11,300 cal yr B.P., suggesting temporal equivalence with the North Atlantic Younger Dryas climatic reversal (12,940 ± 260 – 11,640 ± 250 cal yr B.P.; Alley et al., 1993). A ~500-yr interval of high rock-flour flux in the cores records an early Neoglacial advance between ~3300 and ~2800 cal yr B.P. that was less extensive than the subsequent LIA advance. Steady-state equilibrium-line altitudes (ELAs) for Brynhild and Brisingamen advances estimated with accumulation-area ratio and balance-ratio methods are distinct but nearly indistinguishable at ~2355 m, roughly 200 m below the modern ELA. Conditions required to form and sustain the Brisingamen and Brynhild paleoglaciers include a summer temperature depression of ~3° C, an increase of ~90 cm water-equivalent in winter precipitation, or, more likely, some lesser combination of the two. These constraints imply a local climate that could support only small-scale advances in both the latest Pleistocene and late Holocene, and warmer as well as drier conditions throughout the early Holocene.

Acknowledgements

I would like to thank the following people who assisted in all aspects of the work that culminated in this thesis. My thesis committee; Douglas Clark, Bernard Housen and Chris Suczek; All the people that assisted me in the field and office, and those who provided moral support; Gabriel Cisneros, Galen Ward, Ben Cashman, Joel Cornwall, Jay Kinsman, Andrew Morris, Jason Herndon, Alan Maccarone, Chad Hults, The United States Forest Service – Leavenworth Ranger District - Lisa Therrell, Dave and Diane Bilderback, Christopher Bilderback, Stephen Palmer, Sammantha Magsino, Ed and Julie Feldy and my wonderful wife Alexandra Bilderback.

In addition, I would like to acknowledge the following organizations that provided funding: Mazamas, Geological Society of America, Sigma Xi, David A. Rahm Scholarship and Western Washington University Graduate School and Department of Geology.

Table of Contents

List of Figures and Tables

Introduction

Small alpine cirque glaciers have been the dominant form of glaciation in the North American Cordillera for the past 12,000-15,000 years. High-resolution records of past fluctuations of these Holocene and latest Pleistocene glaciers can provide insight into local paleoclimatic changes as well as the regional spatial and temporal patterns of glacial fluctuations. Glaciers expand and contract in response to climatic factors such as summer temperature and winter precipitation and can therefore be used as paleoclimatic indicators (e.g., Porter, 1981; Matthews and Karlen, 1992; Clark and Gillespie, 1997). Although local exceptions exist, records of Holocene glacier activity in most regions are only broadly constrained. This limited understanding reflects the difficulty of obtaining continuous and accurately dated records of advances and retreats in these usually remote regions. Holocene moraines in the western U.S. rarely contain datable organic material. Also, exposure dates on Holocene landforms based on in-situ cosmogenic nuclides usually suffer from low resolution because of large signal-to-noise ratios in young samples and uncertainties with production rates (e.g., Clark et al., 1995).

In this study, we establish a continuous radiocarbon- and paleomagnetic-controlled time series of glacial fluctuations in the Enchantment Lakes Basin, North Cascades, Washington, since the retreat of the large Pleistocene glaciers. We use paleomagnetic techniques combined with more traditional AMS radiocarbon dating and tephrochronology of lake sediments to provide a continuous proxy of fluctuations of the adjacent cirque paleoglaciers in the Enchantment Lakes Basin. Previous studies have shown that lake sediments can yield high-resolution temporal constraints based on secular variation of the Earth's magnetic field (Lund and Barnerjee 1985; Verosub et al., 1986; Ridge et al., 1990; King and Channell, 1991). To estimate past temperature and precipitation conditions associated with the glacial fluctuations, we reconstructed equilibrium glacial snowlines related to moraines formed during local Holocene glacial maxima.

Geologic Setting

The Enchantment Lakes Basin, located in the Alpine Lakes Wilderness southwest of Leavenworth, Washington (Fig. 1), provides an excellent location to study the Holocene glacial geology of the northeastern Cascades because the basin includes a number of alpine and sub-alpine tarns that adjoin two moraine sets hypothesized to be Holocene-age (Waitt et al., 1982). In addition, the basin is dominated by scoured, granitoid bedrock, which reduces the potential for "old" carbon that might systematically affect radiocarbon dates in lake sediments. During the last glacial maximum, all but the highest peaks of the Enchantment Lakes Basin were glacierized under an

extensive ice field. The last glacial maximum in the Leavenworth area was characterized by two major advances of nearly equal extent, the first between about 24,000 and 22,000 ^{36}Cl yr ago, and the second ending about 17,000 ^{36}Cl yr ago (Swanson and Porter, 1997). Following these advances, the ice flowing from the Enchantment Lakes Basin retreated into the valleys south of Icicle Creek (Fig. 1). About 14,000 to 13,000 ^{36}Cl yr ago, Enchantment Basin glaciers reached the confluence with Icicle Creek during the Rat Creek advance (Swanson and Porter, 1997) and then retreated again and perhaps disappeared as global climate warmed into the early Holocene Hypsithermal period. Globally, the Hypsithermal period reached peak temperatures of probably two or three degrees Celsius warmer than current mean global temperatures about 6,000 years ago (Denton and Porter, 1970). The Hypsithermal period lasted until about 4,500 years ago when global climate began to cool, resulting in a series of small glacier advances around the world, known as the Neoglacial Period (Denton and Porter, 1970). The most recent of these small glacier advances, the Little Ice Age (LIA), began about 700 years ago, reached a maximum in most regions about 100-200 years ago, and ended at the beginning of the 20th century (Grove, 1988).

The Enchantment Lakes Basin contains two well-preserved sets of moraines. These moraines record periods when climate was substantially colder and/or wetter than present. Waitt et al. (1982) argue that the inner belt of moraines (Brynhild moraines) are LIA equivalent based on the absence of a 475 cal yr B.P. Mount St. Helens tephra (W_n) on the moraines and the glacially scoured surface inside the moraines. This inner belt of moraines therefore provides a means to test the timing of the LIA maximum in the Washington Cascades. The timing is important for establishing local climatic patterns.

The outer moraine belt (Brisingamen moraines) is substantially older than the inner moraines based on relative weathering characteristics and the presence of the ~6800 ^{14}C yr B.P. Mount Mazama ash in the meadows inside these ladforms (Waitt et al.,1982). Waitt et al. (1982) contend that these moraines are early Holocene rather than latest Pleistocene on the basis of qualitative weathering characteristics. However, the only numerical constraints for the advance indicate that it is older than ~6800 ^{14}C yr B.P. and younger than about 13,000 ^{36}Cl B.P. (Rat Creek Advance). The distinction between whether the Brisingamen moraines are early Holocene or latest Pleistocene is important to paleoclimatic studies because the early Holocene has generally been regarded as a time of warmth and regional glacier retreat. If the outer moraines are early Holocene, they might indicate significant climatic fluctuations at the onset of the Hypsithermal interval in northwestern Washington (e.g., Beget, 1981 and 1983), a situation perhaps analogous to modern climate trends. Conversely, if the outer moraines are latest Pleistocene, they should record the nature of the transition between the

last glacial maximum and the Hypsithermal interval, perhaps relating to the North Atlantic Younger Dryas interval (e.g., Davis, 2003 and 1994, and Zielinski and Davis, 1987)

Methods

Mapping

We mapped glacial deposits in the upper Enchantment Basin and the surrounding areas at 1:24,000 scale through combined field investigation, aerial photo interpretation, and a laser theodolite survey. Our mapping refines previous mapping by Waitt et al. (1982). We distinguish moraines based on stratigraphic position, moraine preservation, extent of weathering, and the degree of lichen and tree growth. Two distinctive moraine belts, Brynhild and Brisingamen, occur in the Enchantment Lakes area. Brynhild moraines lie inside the Brisingamen moraines and are broad, fresh, multi-crested moraines that exhibit little or no post-depositional erosion, boulder weathering, or tree growth, and lichen growth is minimal. Brisingamen moraines, by contrast, are low-volume moraines that support significant tree and lichen growth. In addition, significant grus, tephra, and organic material accumulated in the meadows behind the Brisingamen moraines in the upper Enchantment Basin.

In addition to minor refinements to the mapping of Waitt et al. (1982), our mapping identified Brynhild and Brisingamen deposits and trim lines to the west, north and east of the upper basin (Fig. 2). Substantial refinements of the area previously mapped by Waitt et al. (1982) include three-dimensional mapping of the moraines using a laser total station (Appendix 1, Bilderback, 2004) and collection of additional striation data (Fig. 2).

Sediment Coring

The lake sediment cores that form the primary data set for this study were collected from five lakes in the Enchantment Lakes Basin during the spring of 2000 and 2001(Appendix 1, Bilderback, 2004). Twelve continuous, 3-inch diameter lake cores ranging in length from 1 to 3 meters were acquired using a modified version of the percussion Reasoner corer (Reasoner, 1993). Cores from Lake Viviane, Crystal Lake and Lake Inspiration (Fig. 2) are presented in this paper. The main modifications to the Reasoner corer made for this study are the replacement of a core catcher with a double O-ring piston, to reduce sediment disturbance, and the doubling of the hammer length, to facilitate coring through unusually dense, thick Mazama tephra.

Cores were collected in the spring while the lake surfaces were still frozen. The cores were collected vertically and were azimuthally unoriented. After extraction, the cores were cut into

approximately 1-meter sections, capped, and sealed for transport out of the field. The cores were kept vertical until sampling to reduce post-coring disturbance of the sediments. At Western Washington University, the cores were stored in a refrigerated room at 4° C. During or after transport, most of the core sections experienced 3-10 cm of settling and dewatering. Integrity of fine stratigraphic horizons in the cores, however, indicated that this settling was fairly uniform and did not disrupt the stratigraphy.

In the lab, we split the cores with a 1.5-meter long demagnetized stainless steel knife, reducing disturbance of remanent magnetism of the sediments. The visual stratigraphy of the cores was logged, photographed, and sampled for ^{14}C AMS dating and other core analyses.

Sediment Analysis

The two main goals of our core analyses are to identify periods of glacial vs. non-glacial sedimentation in the basin, and to date the sediments associated with those periods. Analyses of the lake sediment cores include magnetic susceptibility, organic content (through loss-on-ignition), particle size analysis, magnetic grain size, anhysteretic remanent magnetization (ARM), paleomagnetic field secular variation, tephra identification, and AMS radiocarbon dating.

Magnetic Susceptibility

Magnetic susceptibility (k) measurements provide a rapid, quantitative measure of how magnetic a sample is (Watkins and Maher, 2003). Depending on local bedrock lithologies and depositional environment, higher k typically corresponds to greater abundances of clastic sediment (e.g., rock flour or Aeolian dust), whereas low k indicates greater organic content (e.g., Benson et al., 1996, Bischoff et al., 1997, and Armour et al., 2002). Bulk sediment mass-normalized magnetic susceptibility (χ) was measured on an AGICO KLY3-S anisotropy of magnetic susceptibility bridge. Measurements were made on 8 cm^3 cubes of sediment taken every 4 cm down core. The use of the magnetic susceptibility bridge and discrete samples eliminated the strong influence that tephra layers in lake cores can have on the measurements of adjacent sediments, when a core-scanning susceptibility meter is used. This is important for isolating sedimentary contacts when high χ materials (tephra) are juxtaposed against very low χ materials. Susceptibility measurements were also made on as wide a compositional range as possible of unweathered bedrock samples from the upper Enchantment Basin to gain an understanding of the possible range of χ from bedrock-derived materials.

Loss on Ignition

Burning sediment samples (loss on ignition - LOI) provides a measure of the organic content at different horizons in the lake cores. We measured LOI using sediment samples of 8 cm^3 collected every 4 cm down core. The wet sediment samples were weighed, dried at ~100° C overnight, cooled in a desiccator, and then reweighed. To burn off the organics, the dry samples were placed in ceramic crucibles and baked in a muffle furnace at 500° C for 4 hours. Because LOI can be strongly dependent on the exposure time (Heiri et al., 2001), we choose a burn time of 4 hours instead of the standard 1-hour. After the burn, the sample ash and crucibles were cooled in a desiccator and then reweighed. The percent mass difference between the dry sample weight and the ash closely approximates the percent organics present in each sample.

Particle size analysis

The particle size analyses of lake sediments can provide detailed proxy records of changes in sediment sources. Approximately 1-cc sediment samples were collected at least every 4 cm down core. Locally, samples were collected at shorter intervals in order to assess changes evident in the visual stratigraphy. The goal of the particle size analysis is to assess changes in clastic particle sizes relating to changing sources and energies of sediment production and transport.

The sizes of organics in lake sediments do not directly relate to the energy of the depositional environment and they need to be removed from the sediments before particle size analysis. In order to isolate the clastic sediments, organics in the sediments were chemically removed with a 30% hydrogen peroxide pretreatment. Similarly, diatoms also interfere with clastic grain-size analysis, and must be removed if they occur in abundance. Diatom abundance in the sediments was assessed by counting diatoms in several discrete samples from the longest Lake Viviane core. Diatoms were not removed from any of the lake cores because at their peak abundance they represented only about 4% by volume of a given sediment sample in the Lake Viviane core.

Particle size was analyzed with a Malvern Mastersizer 2000, which has a nominal analytic range of 0.02 to 2000 microns. A small amount of calgon was added to the samples before measurement to facilitate dispersion. Samples were introduced into the Mastersizer dispersion unit using an autosampler, which eliminates subsampling bias. Two or three aliquots of each sample were measured, depending on sample abundance, and each aliquot was measured 3 times. All aliquots of each sample were combined to produce an average measurement for each sample. For rare cases in which a sample had an extreme outlier compared to the other aliquots or the second aliquot did not contain enough sample to be properly measured, the outliers were excluded from the final sample

average.

Magnetic Grain Size and Anhysteretic Remanent Magnetization

We used anhysteretic remanent magnetization (ARM) to further investigate magnetic mineral concentration and partial anhysteretic remanent magnetization (pARM) as a proxy for magnetic grain size (Jackson et al., 1988). We made pARM measurements in each of three representative cores on 8 cm^3 cubes of sediment taken every 4 cm down to about the Mount St. Helens Y_n tephra (3780 cal yr B.P.; Mullineaux, 1986). Partial ARM measurements were made by imparting a DC bias field (0.5 mT) between two specified values of a decaying alternating field and then measuring the resulting remanence. The pARMs and ARMs were imparted using a D-Tech D-2000 af demagnetizer, and the resulting magnetizations were measured with a 2-G Enterprises 755 superconducting rock magnetometer. The results are displayed as a ratio between 10 mT-wide coercivity windows centered on 15 and 85mT for each sample. The remanence of magnetic grains at a specific coercivity window is highly size dependent; the 10-20 mT range will preferentially magnetize magnetite of 5-10 micron size, and the 80-90 mT range will preferentially magnetize much smaller (1 to 0.1 micron) magnetite (Jackson et al., 1988). High values of the ARM 15/ARM 85 ratio represent larger magnetic grain sizes and small values represent smaller magnetic grain sizes.

For the Lake Viviane and Crystal Lake cores, remanence was measured using incremental coercivity windows from 0 to at least 125 mT. When the remanence for each coercivity window is added together the result is the total anhysteretic remanent magnetization (ARM) for each sample. Total ARM, in contrast to magnetic susceptibility, provides a measurement of the concentration of just the magnetic Fe-Ti oxide grains in a sample. In order to best compare ARM samples to each other within and between lake cores, all ARM results presented in this paper are mass normalized. Only coercivity windows centered on 15 and 85mT were measured for the Lake Inspiration core, so a direct measurement of total ARM was not possible for this core. A comparison between the total ARM vs. depth curve and the sum of the measured remanence at the 10 mT coercivity windows centered on 15 mT and 85 mT vs. depth curve for Lake Viviane (Fig. 3) and Crystal Lake shows that the 15 mT plus 85 mT curve and the total ARM curve correlate strongly. We use the mass normalized 15 mT plus 85 mT vs. depth curve for Lake Inspiration as a proxy for total ARM.

Paleosecular Variation

To help refine the age models of our cores, and to aid correlation to other published records, we analyzed paleomagnetic field secular variation (PSV) in cores from Lake Viviane and Crystal

Lake. Verosub et al. (1986) have documented the value of such core analyses for these purposes. Discrete PSV samples were collected at 4 cm intervals by pressing 8 cm^3 plastic cubes into the middle of the split cores. The carrier of most of the remanence in the field area bedrock, and probably the lake sediments, is magnetite (Housen et al., 2003).

In order to identify any post-depositional disturbance of the sediments, not visually apparent in the lake cores, and to estimate the quality of the paleomagnetic record preserved in the sediments, Anisotropy of Magnetic Susceptibility (AMS) was measured with an AGICO KLY3-S susceptibility bridge. In lacustrine depositional environments elongate particles will tend to settle subparrallel to the lake bottom. Since magnetic susceptibility is usually at a maximum parallel to the long axis of detrital magnetic grains, the inclination of the maximum susceptibility axis of the lake's sediment should be close to horizontal and the inclination of the minimum susceptibility axis should be close to vertical. In addition, the magnetic susceptibility ellipsoid for lake sediments should be oblate with maximum (K1) and intermediate (K2) susceptibility axes lying in the bedding plane and the minimum axis (K3) near vertical. We assessed possible disturbance in the Lake Viviane and Crystal Lake cores using both the K3 inclinations (e.g., Rosenbaum et al., 2000) and the shape of the magnetic susceptibility ellipsoid (e.g., Schwehr and Tauxe, 2003) for each PSV sample.

Natural remanent magnetization (NRM) of the samples was measured with a 2-G Enterprises Model 755 cryogenic magnetometer. Samples were measured after progressive alternating field (AF) demagnetization at 2.5 mT steps up to 25 mT, samples were then measured at 5 mT steps up to 55 mT and at 10 mT steps up until they had lost at least 90% of their initial remanence (e.g., Fig. 4). The magnetization components were defined visually with the aid of orthogonal vector plots (Fig 4). Directional components of magnetization were determined using principle component analyses (PCA, Kirschvink, 1980). Two magnetization components were generally present. The first-removed component was generally isolated between 2.5 and 10 mT demagnetization steps. The second-removed component was isolated between the 10 and 90 mT demagnetization steps (Fig. 4)(Appendix 2, Bilderback, 2004).

Tephra Identification

Tephras in the lake cores form distinctive light grey layers and contain abundant microscopic glass shards. The tephras present in the Enchantment area were originally identified by Waitt et al. (1982) as the Mount St Helens W_n Mount St Helens Y_n, and the Mount Mazama tephras; we identify them in our cores based on stratigraphic position and ages of adjoining radiocarbon dates.

^{14}C Dating

Discrete bulk sediment samples and macrofossils, including wood and plant material, were collected from the sediment cores immediately after the cores were split for AMS-radiocarbon analyses. The samples were dried and stored in glass vials before analysis. The samples were analyzed at the Center for Accelerator Mass Spectrometry, Lawrence Livermore National Laboratory. All but two of the analyses presented here are of macrofossils. The exception is of organic-rich gyttja. To assess the validity of the bulk samples, we analyzed adjacent bulk and macrofossil samples from several horizons.

Equilibrium Line Altitude Estimates

Equilibrium line altitudes (ELA) are determined by net accumulation and net ablation, which in turn depend on climatic conditions, glacial surface topography, hypsometry, and glacier aspect (Torsnes et al., 1993). In most locations winter precipitation and summer mean temperature are the main climatic factors that influence accumulation and ablation (Sutherland, 1984). The position of the ELA is thus a climatically sensitive parameter that can be used to estimate the climatic conditions in which the glacier existed.

Steady-state ELAs for the Colchuck and upper Enchantment Basin Brynhild ice limits and for all mapped Brisingamen ice limits were estimated using both an accumulation area ratio (AAR) of 0.65 and a net-balance ratio of 2 (Furbish and Andrews, 1984). The measurements for these methodologies are based on iterative topographic reconstructions of the paleoglacier surfaces using our mapped ice limits (trim lines, erratics, moraines) and maintaining ice thicknesses capable of flow (e.g., Porter, 1975). If the two methods were in close agreement the AAR was used. All but one of the ELAs reported in this study are derived from the AAR method. The AAR method of estimating ELAs of paleoglaciers is more commonly used and less time consuming than the balance-ratio method; however, it is best suited for glaciers with simple hypsometries (which most of the paleoglaciers in the Enchantment Basin have) and can provide poor ELA estimations for glaciers with complex hypsometric distributions. The north Enchantment Brisingamen paleoglacier (Fig. 5) is the only reconstructed glacier in the study area with a complex hypsometry (skewed toward high glacial elevations) that is more appropriate for the balance-ratio method. The upper Enchantment Basin Brynhild and Brisingamen paleoglaciers were divided into two discrete glaciers along an ice divide, based on flow indicators, in order to achieve more meaningful ELA estimates for these glaciers (Fig. 5). The eastern-most paleoglaciers created by this split were used for ELA estimation because they had unconfined flow paths making them good candidates for area-based (AAR) ELA

estimation. The western-most paleoglaciers flowed into a confined bedrock bowl giving them a very limited distribution of elevations. The estimated ELAs of the western-most paleoglaciers are a poor indicator of paleoclimate because of this characteristic.

Climatic Change Estimates

The magnitude of climate change needed to form and sustain the Brisingamen and Brynhild paleoglaciers was estimated following Leonard (1989). The modern summer mean temperature and water-equivalent winter accumulation for the Enchantment Lakes Basin at the calculated paleo-ELAs of the Brynhild and Brisingamen paleoglaciers were extrapolated from linear lapse rates calculated from lower-altitude weather data. The summer mean temperature regression was calculated using temperature data from 1993-2002 from nine sites around the study area ranging in altitude from 344 m to 1640 m. The summer mean temperature regression is statistically significant ($p = 0.005$) and altitude explains 82% of the variance in summer temperature. Winter precipitation is not as well correlated with altitude as temperature is (Leonard, 1989). In addition, in the Cascades, the dominant winter weather pattern is movement of moisture from west to east off the Pacific Ocean. This weather pattern influences the relationship between winter precipitation and altitude. At the same altitude, the west side of the Cascades receives far more precipitation than the east side of the range. In order to account for the effect the Cascade rain shadow, only weather stations east of the Cascade crest, approximating the precipitation regime of the field area, were used to calculate the winter precipitation lapse rate. The modern winter precipitation regression was calculated using winter precipitation data from 1993-2002 from seven sites east of the cascade crest around the study area ranging in altitude form 344 m to 1640 m. The winter precipitation regression is statistically significant ($p = 0.02$), and altitude explains 70% of the variance in winter precipitation.

Because the ELAs in this study are above the highest weather station, the lapse rates had to be extrapolated. From these extrapolations, the predicted climate at the ELAs of the Brynhild and Brisingamen paleoglaciers were plotted on a graph of winter accumulation versus summer mean temperature. This graph (Fig. 6) includes climates at the ELAs of modern glaciers from around the world that define an envelope of winter accumulation and summer mean temperature within which glaciers form. To estimate the change in climatic conditions that would sustain the Brynhild and Brisingamen paleoglaciers, the extrapolated modern climate at the ELAs of the paleoglaciers was shifted into the envelope of modern glacier conditions (e.g., Leonard, 1989).

Results

Age Constraints

The age constraint for the sediments from the lake cores is provided by four dating methodologies: tephra chronology, AMS ^{14}C, correlation with ^{14}C dated paleosecular variation curves, and age interpolation based on sedimentation rates between dated horizons. There are three major tephra marker beds in the lake cores: the Mount St Helens W_n and Y_n tephras and the tephra deposited by the climatic eruption of Mount Mazama. The Mount St Helens W_n tephra is 475 cal yr B.P. (AD 1480) dated by dendrochronology (Yamaguchi, 1983). The Mount St Helens Y_n tephra is 3780 cal yr B.P. (3510 ± 80 ^{14}C yr BP) (Mullineaux, 1986). The Mount Mazama eruption is dated at 7627 ± 150 cal yr B.P. (Zdanowicz et al., 1999). AMS ^{14}C dates are from macrofossils and two bulk-sediment samples, from the pre-Mazama section of the Lake Viviane core, and from the Crystal Lake core (Fig. 7a and 7b) (Appendix 3, Bilderback, 2004). Where AMS ^{14}C dates were not done, clastic horizons are constrained by interpolated sedimentation rates between dated horizons in Crystal Lake and Inspiration Lake (Fig. 7b and 7c).

The AMS sediment disturbance evaluation of the post-Mazama section of the Lake Viviane core shows that K3 is nearly vertical and that the shape of the magnetic susceptibility ellipsoid is oblate between about 10 and 75 cm depth (Fig. 8). Over this interval the average inclination of K3 (INC_{k3}) is 80.5 and the standard deviation of K3 inclinations (STD_{k3}) is 4. Rosenbaum et al. (2000) found that an INC_{k3} of greater that about 81 and a STD_{k3} less that about 6.5 generally indicates very little deformation in a sediment core. The shape of the magnetic susceptibility ellipsoid was determined from our AMS data by calculating the shape factor (T) following Jelinek (1981) (Fig. 8). Schwehr and Tauxe (2003) demonstrated that undeformed sediments generally exhibit an oblate magnetic susceptibility ellipsoid rather than a triaxial or prolate ellipsoid. Using the criteria of Rosenbaum et al. (2000) and Schwehr and Tauxe (2003) as a guide, we submit that the 10 to 75 cm depth interval in the Lake Viviane core suffered very little post depositional disturbance. In contrast to the Lake Viviane core, the AMS data indicate that the Crystal Lake core suffered extensive post deposition disturbance. For the Crystal Lake core the INC_{k3} is 55, the STD_{k3} is 29 and about 39% of the samples exhibited a prolate or triaxial magnetic susceptibility ellipsoid. The Crystal Lake core does have intact visual stratigraphy, but the AMS data shows that it is unusable for paleomagnetic studies.

The post-Mazama section of the Lake Viviane core is dated by correlation of its PSV record (Fig. 9) to the ^{14}C-dated PSV record in Fish Lake, Oregon (Verosub et al., 1986). The Lake Viviane core was not azimuthly oriented during coring. In order to compare the declination curves from Lake

Viviane and Fish Lake, we attempted to orient the Lake Viviane PSV record by calculating the mean declination for the time period between the Mount St Helens Y_n tephra and the Mount St Helens W_n tephra for the Lake Viviane core and comparing that to the mean declination for the same time period from the Fish Lake PSV record. The difference between the two mean declinations, over the same time period, was used to orient the Lake Viviane PSV record with respect to the Fish Lake PSV record. Even with this azimuthal reorientation, however, the declination curve from Lake Viviane does not correlate well with the Fish Lake curve or the Hagstrum and Champion (2002) volcanic rock derived declination curve (Fig. 10). The inclination curve, on the other hand, does show good correlation with the other curves (Fig. 10), and the Lake Viviane inclination curve was used to derive a PSV-correlated age model for the post-Mazama sediment of the Lake Viviane core (Fig. 7a and 10).

The PSV-correlated age model for the post-Mazama sediment of the Lake Viviane core was obtained by using the AnalySeries time-series analysis program (Paillard et al., 1996) to transform the Lake Viviane inclination versus depth curve (Fig. 9) into an inclination versus age curve using the Fish Lake inclination curve as the reference signal. In this process, major spikes and troughs in the inclination curves as well as both the Mount St. Helens tephras were used as tie-points between the curves; a constant sedimentation rate was assumed between tie-points (Appendix 4, Bilderback, 2004). The correlation coefficient between the unadjusted Lake Viviane curve and the Fish Lake curve is 0.786, and the correlation coefficient between the adjusted Lake Viviane curve and the Fish Lake curve is 0.856, with a correlation coefficient of one (1) representing perfect correlation and negative one (-1) representing perfect inverse correlation. The process for creating the Lake Viviane PSV age model is qualitative, but does provide a reasonable first order age model. We used the Fish Lake curve (Verosub et al., 1986) instead of the volcanic rock curve (Hagstrum and Champion, 2002) to compile the post-Mazama age model for the Lake Viviane core because the depositional process that resulted in a record of PSV is most similar for the Lake Viviane and Fish Lake records.

Lake Sedimentology

The focus of the lake sedimentology is on grey clastic horizons that represent sedimentary environments distinct from the more organic or tephra rich horizons that dominate the lake cores (Fig. 7a, 7b and 7c). Two distinct post- Mount St Helens Y_n clastic intervals appear in all of the cores and are characterized by low χ, low ARM, trends toward lower organic percentages, a smaller particle size mode, and an increase in the relative proportion of clay- and silt-sized particles that make up the sediments (Fig. 7a, 7b and 7c). In addition to these characteristics, the magnetic particle size ratio of pARM 15mT/85mT generally decreases coincident with the clastic intervals and reaches a low point

in sediment overlying the clastic intervals. The younger post- Mount St Helens Y_n clastic interval is conspicuously interrupted by the Mount St Helens W_n tephra; however, the pre and post W_n intervals of this sediment appear to have consistent sedimentary characteristics.

Only the Lake Viviane core penetrated the extremely thick Mazama tephra and recovered pre-Mazama organic and clastic sediments. The pre-Mazama sequence includes about 35 cm of highly organic sediment, which overlies an unknown thickness of grey clastic sediment (Fig. 7a). Although we cored about a half-meter into the pre-Mazama grey clastic sediment, only five cm were retrieved fully intact (Fig. 7a) due to partial wash-out during extraction from about 40 m of water. This pre-Mazama clastic sediment exhibits χ that is slightly elevated compared to the highly organic interval that overlies it, and the percent organic content in this interval is much lower than the overlying interval. Also, the particle size mode and the relative proportions of clay, very fine sand, and medium sand in this interval are elevated compared to the overlying organic interval.

Equilibrium Line Altitudes

The modern orographic ELA in the upper Enchantment Lakes Basin is close to or above the elevation of the ridge (~2560 m) that defines the southern-most extent of the upper basin paleoglaciers (Fig. 5), because only perennial snowfields, not active glaciers, currently occupy the upper basin. Steady-state equilibrium-line altitudes (ELAs) for Brynhild and Brisingamen advances are distinct in that the Brisingamen glaciers were consistently larger than the Brynhild glaciers, and therefore required a lower ELA; however, the ELA estimates are insensitive to these differences because the bench-like hypsometry of the ablation zones of the glaciers dictates that small changes in ELA can cause substantial changes in glacier extent. Based on our methods, the ELAs of the two advances are therefore statistically indistinguishable at about 2355 m (Table 1, Fig. 5). If the perennial snowfields can be used as an indicator of local ELA, then about a 200 m ELA depression was required to grow the Brisingamen and Brynhild paleoglaciers.

Discussion

Fish Lake, Oregon, provides a robust radiocarbon-constrained master chronology of paleosecular variation for the western U.S. (Verosub et al., 1986; Hanna and Verosub, 1988) and is therefore a reasonable tool for developing age models of similar lake sediments. Unfortunately, without ^{14}C control on the post-Mazama sediments from Lake Viviane, we cannot compare the age model we develop for the core from our PSV data with a more conventional ^{14}C age model. The PSV age model does provide a reasonable first order estimate of numeric ages for the sediments,

however. The Lake Viviane inclination curve agrees well with the Fish Lake and volcanic rock inclination curves (Fig. 10). In addition, the Fish Lake PSV derived Lake Viviane age model indicates higher sedimentation rates during an interval of elevated flux of medium sand and coarser sediments between about 31 and 41 cm depth (Fig. 7a) (Appendix 4, Bilderback, 2004). This provides some support for the adjusted age model because periods of coarser sedimentation (indicating higher energies of transport) probably also experience increased sedimentation rates. It is not known why the inclinations of Lake Viviane samples appear too steep (Fig. 10) compared to the inclinations of the other PSV curves. A sub-vertical core barrel penetrating horizontally bedded lake sediments could, depending on the orientation, result in too steep inclinations. However, for this to explain all the difference between the Lake Viviane inclinations and inclinations of the other PSV curves, the core barrel would have to be tilted about 10 degrees with respect to vertical, and such a tilt would have been evident in the bedding of the split core. This amount of tilt was not evident in the Lake Viviane core (Fig. 7a).

The highlighted intervals of sedimentary and magnetic characteristics in Figures 7a, 7b and 7c exhibit distinctive properties that distinguish them from the other sediment in the cores and suggest that they represent periods of upstream glacial activity. During these periods χ and ARM are relatively low. In contrast to other published studies (e.g., Benson et al., 1996; Bischoff et al., 1997; Armour et al., 2002), the coincidence of clastic horizons and low magnetic signals in the Enchantment Lakes Basin generally indicates increased input of bedrock-derived clastic sediment (rock flour) from the upper basin (Fig. 1). The bedrock in the field area varies from granodiorite in the south, where the paleoglaciers were located, to quartz diorite in the northern part of the Enchantment Lakes drainage (Fig. 2) (Erikson, 1977; Tabor et al., 1982). χ tests done on both of these rock types indicate that ferimagnetic mineral concentration is relatively low (χ between 7.6E-09 to 5.5E-08 m^3/kg). Erikson (1977) documents that the granodiorite phase of the batholith has one to three weight percent less total iron than the quartz diorite, which could result in measurably different χ and ARM. We suggest that low χ and ARM sediment includes a higher proportion of bedrock-derived materials and, furthermore, that the sediments with the lowest χ and ARM are sediments derived mainly from the granodiorite in the southern part of the field area. Particle size analysis indicates that during the periods of low χ and ARM sediment input (in the middle and late Holocene), there was an increase in clay- and silt-sized particles (Fig. 7a, 7b and 7c). Similarly, an increase in clay- and very fine sand-sized particles at the base of the Lake Viviane core (latest Pleistocene) also coincides with low χ (Fig. 7a). The finer grained clastic sediment probably represents increased rock flour production during these periods. The Brisingamen and Brynhild

moraines in the southern part of the field area, upstream from the cored lakes, provide an explanation for the lower organic, low χ, low ARM, and finer grained sediments because during moraine building glacial events, downstream sedimentation would have been dominated by inorganic, low χ and ARM granodiorite rock flower. The relationship between glacial activity and downstream sedimentation has been well established (e.g., Leonard, 1986 a and b; Clark and Gillespie, 1997; Heine, 1998). The magnetic particle size ratio of pARM 15mT/85mT is also an indicator of distinct sediment sources. Magnetic particle sizes decrease during the periods of increased rock flour flux (low χ and ARM) and attain minima following these periods during the middle and late Holocene (Fig. 7a, 7b and 7c). Watkins and Maher (2003) conclude that aeolian dust was the main source of North Atlantic sediments that contain fine-grained magnetic particles. The higher proportion of fine-grained magnetic particles deposited in the cored Enchantment lakes may also indicate a larger aeolian dust constituent during recession, with maxima (low pARM 15mT/85mT ratio) shortly following deglaciation.

The low-χ, low-organic, clay- to very fine sand-sized pre-Mazama sediment in the Lake Viviane core represents distinctive sedimentation that post-dates the Rat Creek advance 14,000 to 13,000 ^{36}Cl yr ago (Swanson and Porter, 1997), and appears to be latest Pleistocene in age. Similarity to late-Holocene sediments clearly related to the LIA outwash, and absence of any other pre-Mazama rock-flour intervals in the cores, indicate that the sediment was probably deposited during the building and retreat from the Brisingamen moraines. The sediments associated with the Brisingamen advance in Lake Viviane are slightly different than those of the middle- and late-Holocene glacial advances (Fig. 7a). Brisingamen sediments in Lake Viviane exhibit very slightly elevated χ, lower organic content, an elevated particle size mode, and an elevated proportion of very fine-sand sized sediments when compared to the middle- and late-Holocene glacial sediments. These differences most likely reflect a greater abundance of loose, coarse-grained sediments following deglaciation after the Rat Creek advance, and the greater size (sediment input) and closer proximity of glaciers to Lake Viviane during the Brisingamen advance (Fig. 2).

Timing of Glacial Activity in the Enchantment Lakes Basin

Sediments in Lake Viviane, Inspiration Lake, and Crystal Lake indicate that there were at least two Neoglacial advances and an older pre-Mazama glacial advance. The sediment from the younger Neoglacial advance (LIA) and the pre-Mazama glacial advance can be positively correlated to the Brynhild and Brisingamen moraines, respectively, based on moraine position in the Enchantment Lakes drainage and association with Mount St Helens W_n, Mount St Helens Y_n and the

Mount Mazama tephras.

The sedimentary record further indicates that the onset of the Brynhild or LIA advance was between 1000 and 800 cal yr B.P. However, this advance did not reach its maximum position until after 475 cal yr B.P. as indicated by the lack of Mount St Helens W_n tephra on or behind the Brynhild moraines (Waitt et al., 1982). The timing of the maximum extent of the Brynhild advance agrees with many other LIA moraines in the region (Heikkinen, 1984; Leonard, 1974; Miller, 1969; Sigafoos and Hendricks, 1961; Burbank, 1981 and Osborn and Luckman, 1988). The lake cores also show that there was an earlier, less extensive, Neoglacial advance in the Enchantment Lakes Basin between ~3300 and 2800 cal yr B.P. This advance does not have associated moraines preserved upstream of the cored lakes, but the sedimentary response during this interval is similar to that during the Brynhild advance (LIA) (Fig. 7a and 7c) and the longer lasting and more extensive Brynhild advance probably overrode and erased any evidence of the moraines of this earlier Neoglacial advance.

The Lake Viviane core indicates that there were no active glaciers upstream of the lake between about 11,160 cal yr B.P. (9715 ± 40 ^{14}C yr B.P.) and the deposition of the Mazama tephra at about 7630 cal yr B.P. (Zdanowicz et al., 1999). In fact, this interval exhibits the highest organic/lowest clastic input of any time period from any core collected in the Enchantment Lakes catchment (Fig. 7a, 7b and 7c). This finding contrasts with work by Heine (1998) and Thomas et al. (2000) from the more maritime settings of Mount Rainier and Mount Baker. Heine (1998) describes an advance on Mount Rainier between about 10,900 and 9950 cal yr B.P. and Thomas et al. (2000) describes an advance on Mount Baker between about 9450 and 8400 cal yr B.P. We see no evidence of such advances in the Enchantment Lakes Basin.

Our constraints on the Brisingamen advance lend further support to the notion that glacier and climate dynamics at the end of the Pleistocene were complex in the Pacific Northwest (e.g., Clark, 2003). The Brisingamen advance ended at ~ 11,300 cal yr BP based on a stratigraphically close AMS ^{14}C date and sedimentation rates of the highly organic sediment at the bottom of the Lake Viviane core (Fig. 7a). This minimum age constraint for the Brisingamen advance, as indicated by the correlated glacial sediment in Lake Viviane, suggests the advance may correlate to the North Atlantic Younger Dryas climatic reversal (12940 ± 260 – 11640 ± 250 cal yr BP; Alley et al., 1993), and that the Enchantment Lakes Basin responded differently during this time than other glaciers west of the crest of the Cascades (Heine, 1998; Thomas et al., 2000; Kovanen and Easterbrook, 2001; Kovanen and Slaymaker, 2004 in review). Heine (1998) argues that there was no glacier advance during the Younger Dryas Chronozone on Mount Rainier, whereas Kovanen and Easterbrook (2001)

indicate that alpine glaciers around Mount Baker advanced during the Younger Dryas climatic reversal, implying the glaciers reached altitudes as low as 150 m in the North Fork Nooksack River. More recently, Easterbrook (2003) and Kovanen and Slaymaker (2004, in review) have modified these interpretations, indicating that the Younger Dryas advance around Mount Baker was significantly less extensive, but still significant (e.g., an ELA depression of 355-400 m relative to modern). Glaciers in the Enchantment Lakes Basin apparently advanced during the Younger Dryas period, but the response was subdued, producing (Brisingamen) glaciers only slightly larger than those that advanced during the LIA (Fig. 2 and 5). Age constraints allow the possibility of similar small-scale glacier advances on and near Mount Baker coeval with the Younger Dryas climatic reversal (Burrows, 2000; Thomas et al., 2000). Matthewes et al. (1993) document evidence for a cool interval during the Younger Dryas Chronozone in terrestrial macrofossils in marine sediments offshore of British Columbia, although the magnitude of the cooling onshore is unclear. The combination of these studies with the new constraints on timing of the Brisingamen advance suggests that climates shifted rapidly both spatially and temporally at the end of the Pleistocene, and that the climatic patterns were not analogous to those of the late Holocene.

Climatic Significance

The similarity of the Brynhild and Brisingamen ELA estimates for the upper Enchantment Lakes Basin reflects both the complexities of local orographic factors, such as slope, aspect, and wind-drift accumulation that lower the local ELA below that of the regional ELA, and the uncertainties inherent to ELA estimates, especially when applied to small cirque glaciers (Meierding, 1982). All of the areas in the Enchantment Lakes Basin occupied by glaciers during the latest Pleistocene and Neoglacial times sit in local ELA depressions based on the presence of current or historic glaciers at a lower elevation than the regional ELA. Because the local orographic effects become progressively less as the glaciers grow beyond the cirques, the Enchantment glaciers will be less sensitive to lowering of the regional ELA than larger valley glaciers that are less affected by local orography. It is apparent, however, that the paleoclimatic perturbation associated with the Brisingamen advance was slightly greater than that associated with the Brynhild advance because throughout the Enchantment Lakes field area, Brisingamen moraines are preserved outside the younger LIA equivalent Brynhild moraines.

To constrain the magnitude of climate change required to produce the Brisingamen and Brynhild paleoglaciers, we compared the modern climate (summer temperature and winter accumulation) at the ELA of the paleoglaciers to the climates at the ELAs of modern glaciers from

around the world that define an envelope of conditions that characterize steady-state glaciers (e.g., Leonard, 1989). We assessed the climate change based on what would be required to bring the Brisingamen and Brynhild ELA climates into the envelop within which glaciers form. This procedure yields two endpoint possible paleoclimate regimes and an intermediate paleoclimatic estimate, which is the smallest possible climatic change required to move the Enchantment Lakes Basin modern climate in to the glacier-forming envelope (Fig. 11). The maximum summer temperature depression and zero winter precipitation increase endpoint is three degrees C below modern mean summer temperature and the maximum winter precipitation increase and zero temperature depression endpoint is a winter precipitation increase of 88 cm water equivalent above modern precipitation. The intermediate paleoclimatic estimate is a mean summer temperature depression of two degrees C and a winter precipitation increase of 26 cm water equivalent. The paleoclimate estimates presented here, while a first order estimate of the climate at the time of glaciation, are probably less precise than those made on larger glaciers that suffer less from error associated with ELA reconstruction and potential local climatic controls.

Conclusions

The sediments recovered from lakes in the Enchantment Lakes Basin record periods of distinct sediment input that can be correlated with upstream glacial activity. Tephra chronology, AMS ^{14}C, correlation with ^{14}C dated paleosecular variation curves, and age interpolation based on sedimentation rates between dated horizons refined the age constraints of the Brisingamen and Brynhild moraine-building glacial advances (Waitt et al., 1982) and a smaller early Neoglacial advance. These lines of temporal evidence in association with the sedimentology indicate that the Brisingamen advance occurred during the North Atlantic Younger Dryas climatic reversal, that glacial advances did not occur in the Early Holocene and that the onset of Neoglaciation in the Enchantment Lakes Basin occurred in the Middle Holocene. The timing and extent of the Younger Dryas equivalent Brisingamen advance in the Enchantment Lakes Basin differs from other studies in the North Cascades that report either a larger glacial response (Kovanen and Easterbrook, 2001; Kovanen and Slaymaker, 2004 in review) or virtually no glacial response (Heine, 1998) during this time period. The Enchantment Lakes Basin did experience a glacial advance that overlaps, at least to some degree, with the North Atlantic Younger Dryas climatic reversal. The response, however, was muted compared to that in the North Atlantic and to an advance proposed at Mount Baker (Kovanen and Easterbrook, 2001; Kovanen and Slaymaker, 2004 in review), producing glaciers with areas about 1.5 to 3 times greater than those associated with the LIA maximum in the basin, and little

change in estimated ELAs. The apparent variability of glacier activity in the North Cascades during the Younger Dryas Chronozone suggests that there may have been significant variability in local climatic patterns at the close of the Pleistocene. This variability may have continued into the early Holocene, with significant glacier advances to the northwest (Mount Baker; Thomas, et al., 2000) and the southwest (Mount Rainier; Heine, 1998), but not in the Enchantments. Alternatively, some of the records from these sites may have been misinterpreted. In contrast to these intervals, late-Holocene glacial expansions in the Cascades appear to roughly coincide in time with each other, with the Holocene maximum being achieved in the late LIA period throughout the North Cascades.

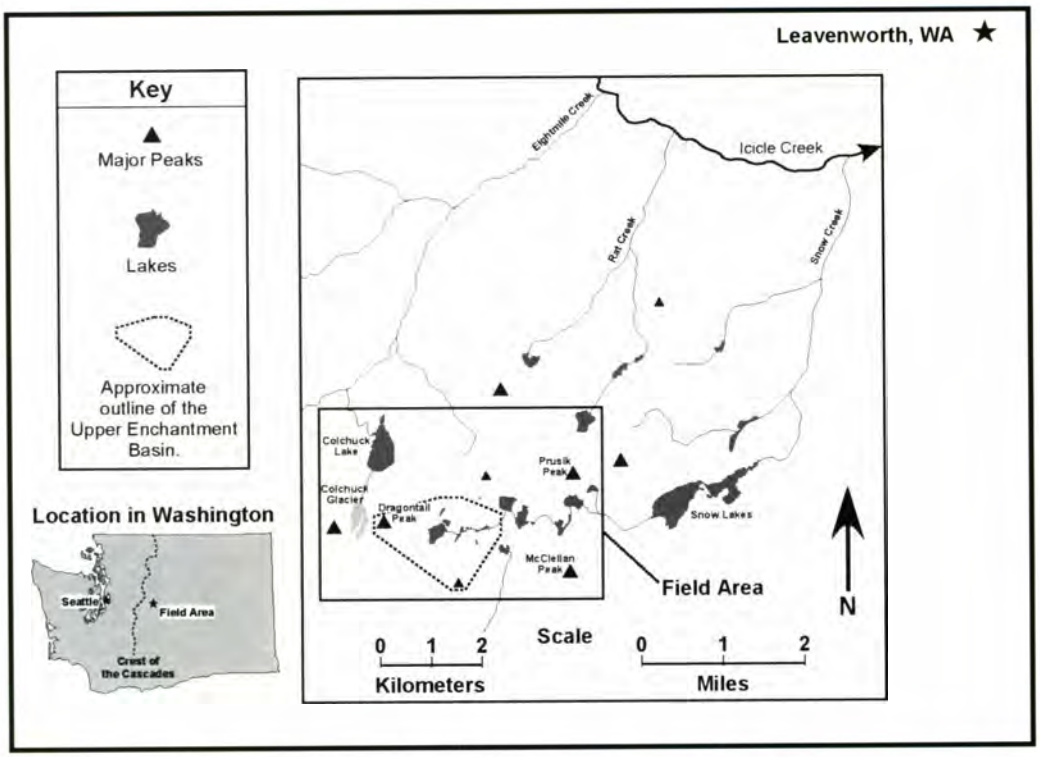

Figure 1. General location map of the field area showing lakes, streams, and major peaks.

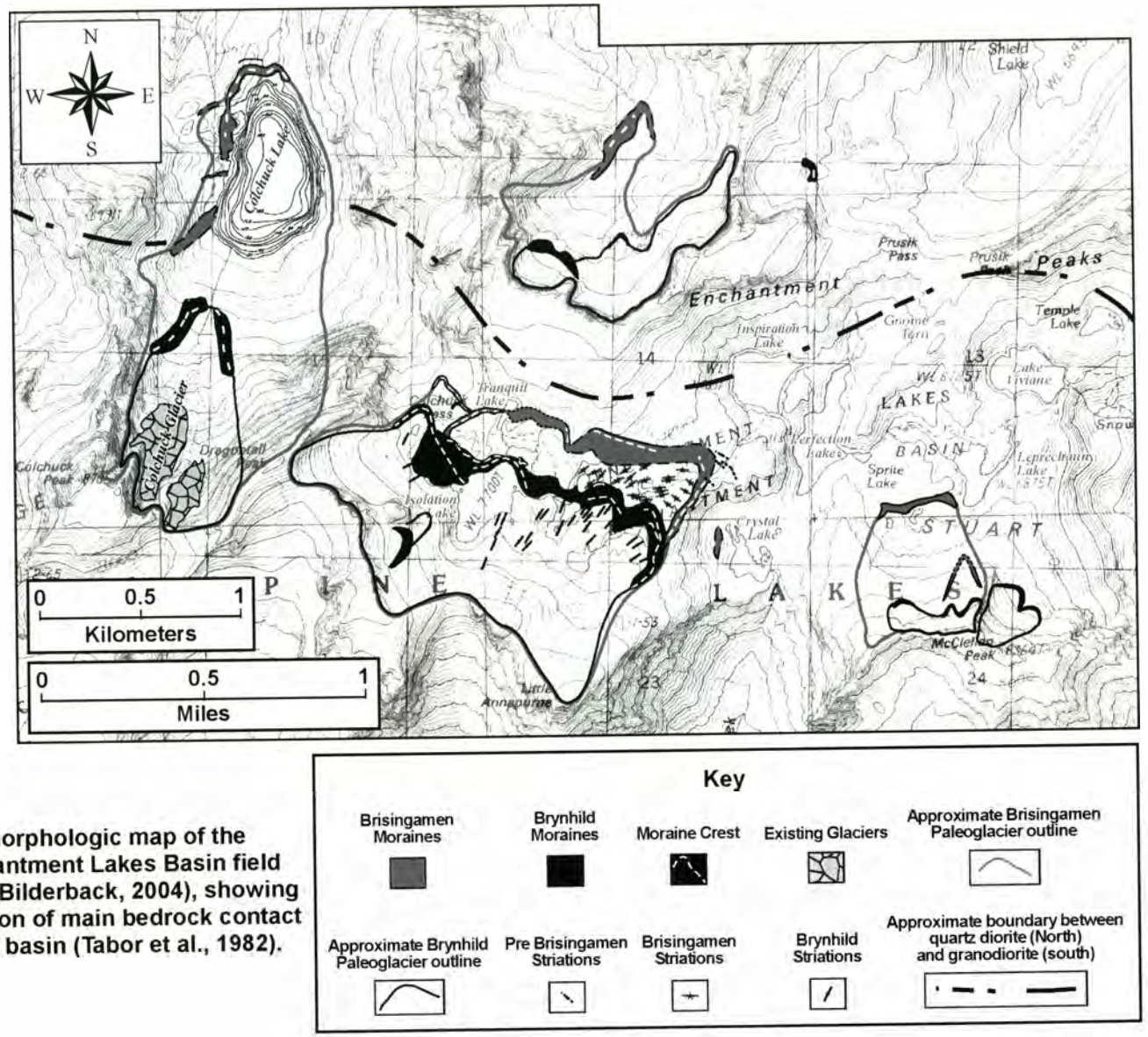

Figure 2. Geomorphologic map of the Enchantment Lakes Basin field area (Bilderback, 2004), showing location of main bedrock contact in the basin (Tabor et al., 1982).

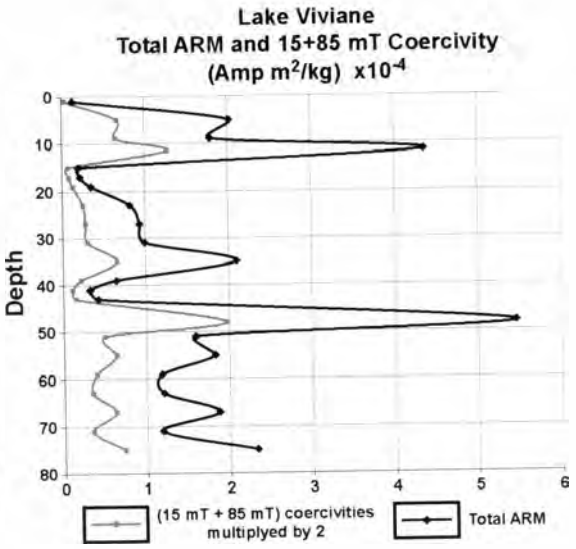

Figure 3. Curves depicting mass normalized total ARM and the 15+85 mT coercivity verses depth for the post-Mazama section of the Lake Viviane core. The 15+85 mT coercivity verses depth curve was multiplied by a factor of 2 to display it at the same scale as the total ARM curve. These curves correspond very well, enabling us to use the15+85 mT coercivity verses depth curve as a proxy for the total ARM curve where complete total ARM data were not collected.

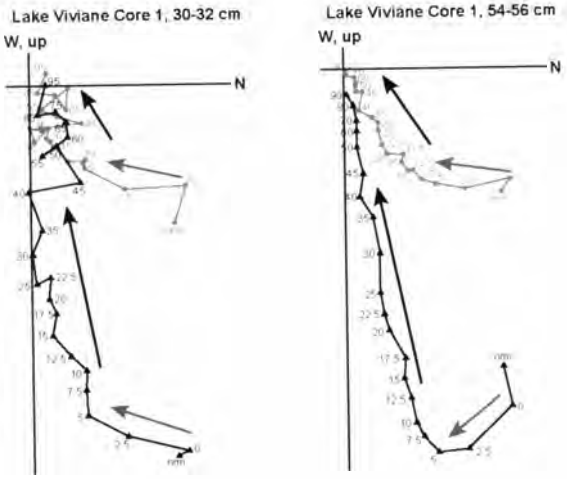

Figure 4. Two alternating-field demagnetization plots for typical Lake Viviane samples. The black path is inclination and the grey path is declination. The demagnetization field strength is noted in mTs for each step along the demagnetization path. The approximate orientations of the first removed components are indicated with grey arrows and the approximate orientations of the second removed components are indicated with black arrows.

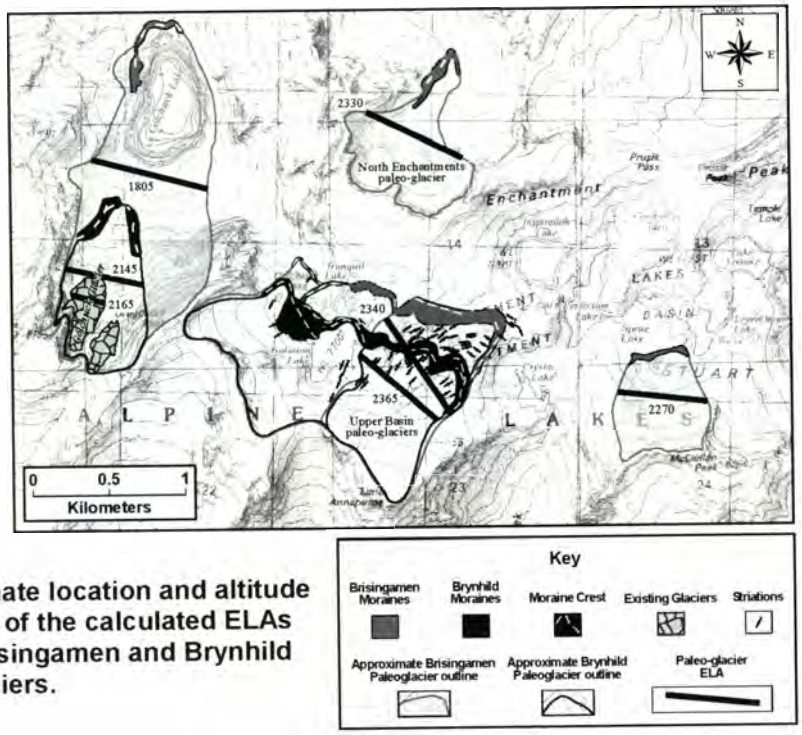

Figure 5. Approximate location and altitude in meters of the calculated ELAs of the Brisingamen and Brynhild paleoglaciers.

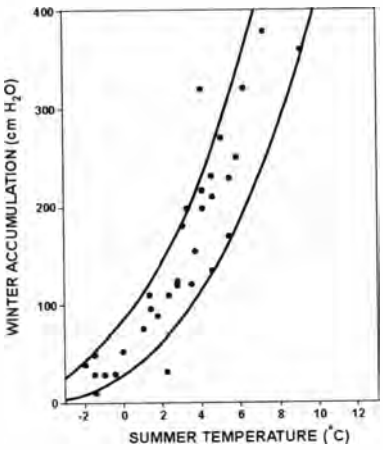

Figure 6. Plot of winter accumulation versus summer mean temperature at the ELA of modern glaciers from around the world. Lines define an envelope of conditions at which modern glaciers exist (Leonard, 1989).

Figure 7a, b, c. Results of sediment analysis of cores from lakes Viviane, Crystal, and Inspiration, respectively. The grey shading in each graph highlights time periods of similar sediment characteristics referred to in the text. The numeric dates listed in black text are ^{14}C dates or tephra dates where indicated. The numeric dates listed in grey text in figure 7a are derived from the Paleosecular variation age model referred to in the text. The numeric dates listed in grey text on figures 7b and 7c are age estimates based on sedimentation rates between ^{14}C dates or tephra horizons.

Figure 7a.

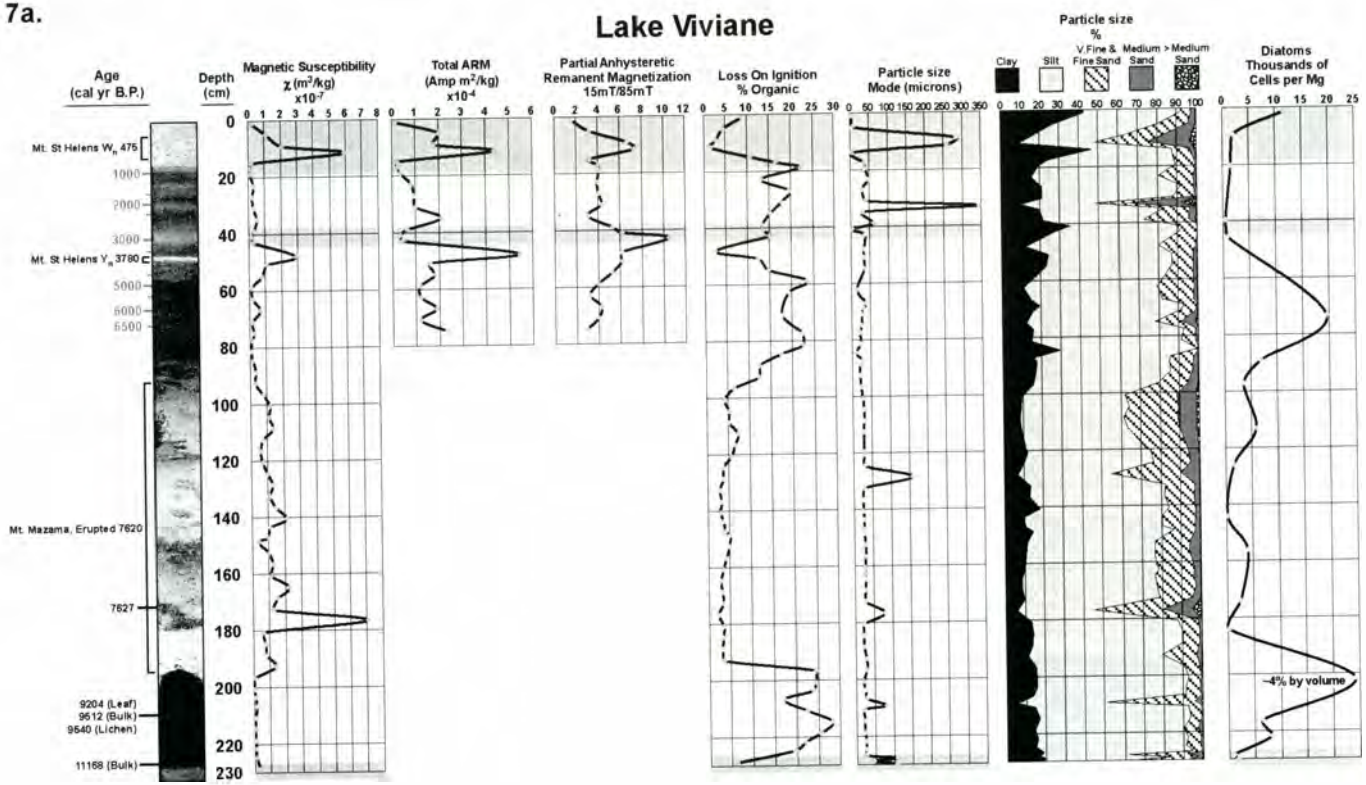

Figure 7b.

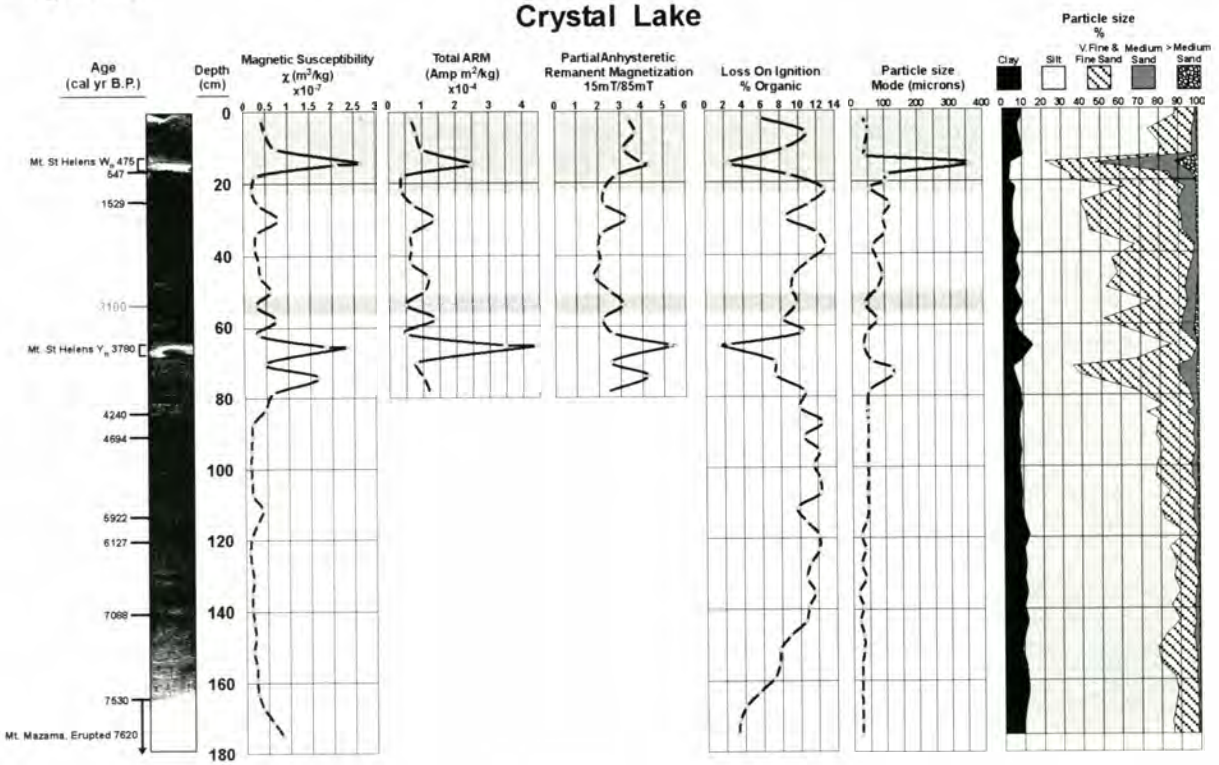

Figure 7c.

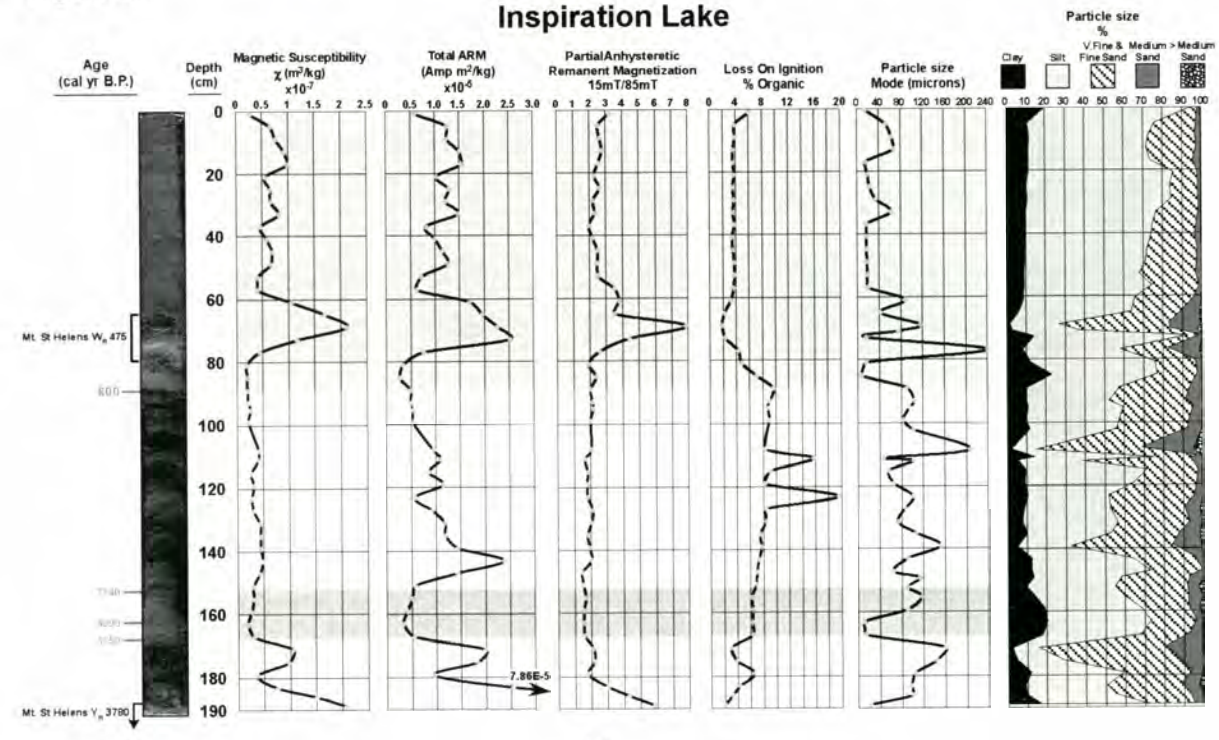

Paleoglacier Name:	ELA (meters)
Brisingamen Colchuck	1805
Brisingamen North Enchantment	2330
Brisingamen Upper Basin	2340
Brisingamen McClellan	2270
Brynhild Colchuck	2145
Brynhild Upper Basin	2365
Modern Colchuck Glacier	2165

Table 1. Table of the ELA estimates for the reconstructed paleoglaciers and the one active glacier (modern Colchuck Glacier) in the Enchantment Lakes Basin Field area.

Figure 8. AMS results from the post Mazama section of the Lake Viviane core. The graph on the left shows the inclination of the K1 and K3 susceptibility axes and the graph on the right shows the shape factor (T) (Jelinek, 1881) of the magnetic susceptibility ellipsoid. The shaded area indicates an area of probable disturbed sediment following Rosenbaum et al. (2000) and Schwehr and Tauxe (2003).

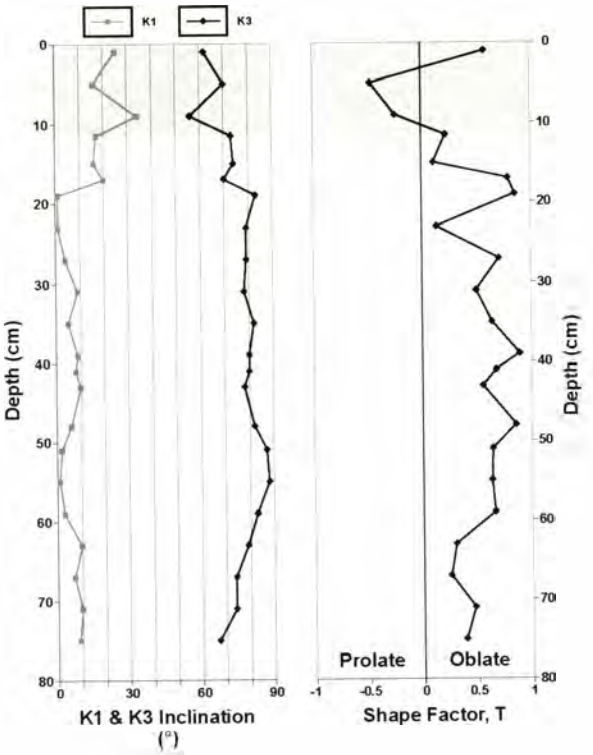

Figure 9. Paleosecular variation curves for Lake Viviane. The mean angular deviation (MAD) is used as a rough error bar for each sample. Where the error bars are not present, the MAD is contained within the plotted points.

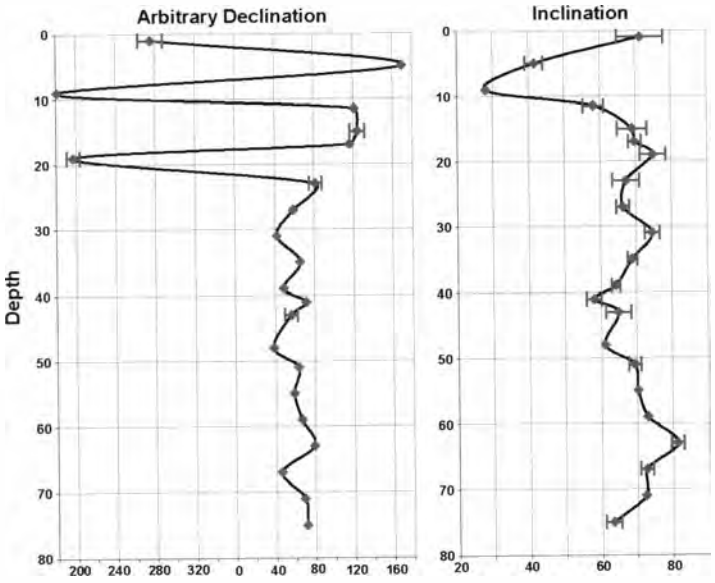

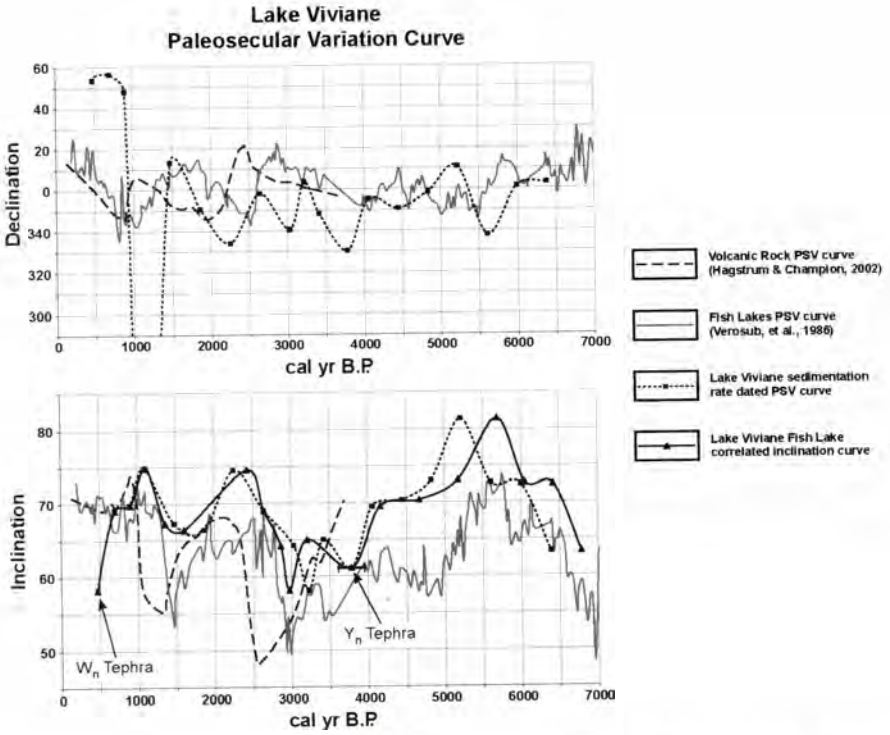

Figure 10. Paleosecular variation (PSV) curves for Lake Viviane plotted against PSV curves for Fish Lake, OR (Verosub, et al. 1986) and a compilation volcanic rock PSV curve (Hagstrum & Champion, 2002), both of which have been recalculated to the latitude and longitude of Lake Viviane. Also noted on the inclination curve, are the Mt. St Helens W_n and Y_n tephras. The Mt. St Helens Y_n tephra calibrated age is plotted with its 2-sigma age range (black bar).

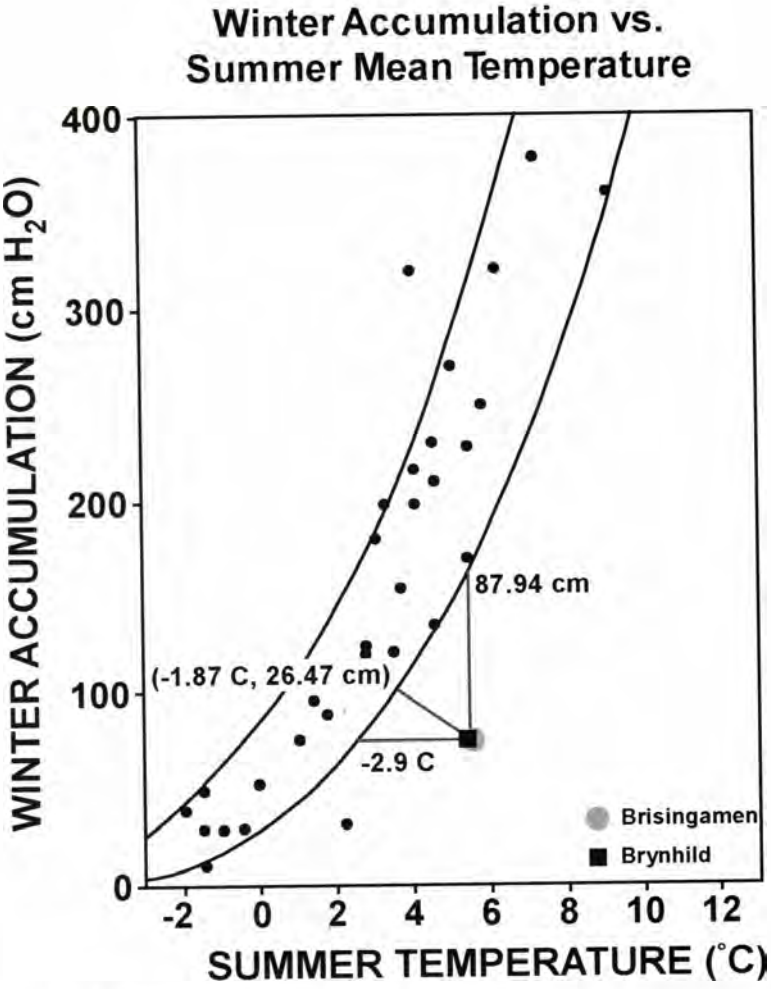

Figure 11. Plot of winter accumulation versus summer mean temperature at the ELA of modern glaciers from around the world. Lines define an envelope of conditions at which modern glaciers exist (Leonard, 1989). Also plotted are modern climatic conditions at the ELAs of the Brisingamen and Brynhild paleoglaciers and potential changes in climate required to shift the Brisingamen and Brynhild paleoglaciers into the glacier-supporting envelope.

References

Alley, R. B., Meese, D. A., Shuman, A. J., Gow, A. J., Taylor, K. C., Grootes, P. M., White, J. W. C., Ram, M., Waddington, E. D., Mayewski, P. A., and Zielinski, G. A., 1993. Abrupt accumulation increase at the Younger Dryas termination in the GISP2 ice core. *Nature*, v. 362: 527-529.

Armour, J., Fawcett, P. J., and Geissman, J. W., 2002. 15 k.y. paleoclimatic and glacial record from northern New Mexico. *Geological Society of America*, v. 30, no. 8: 723-726.

Beget, J. E., 1981. Early Holocene glacier advance in the North Cascade Range, Washington. *Geology*, v. 9, no. 9: 409-413.

Beget, J. E., 1983. Radiocarbon-dated evidence of worldwide early Holocene climate change. *Geology*, v. 11, no. 7: 389-393.

Benson, L. V., Burdett, J. W., Kashgarian, M., Lund, S. P., Phillips, F. M., and Rye, R. O., 1996. Climatic and hydrologic oscillations in the Owens Lake Basin and adjacent Sierra Nevada, California. *Science*, v. 274, no. 5288: 746-748.

Bilderback, E. L., 2004. Timing and Paleoclimatic Significance of Latest Pleistocene and Holocene Cirque Glaciation in the Enchantment Lakes Basin, North Cascades, WA. MS thesis, Western Washington University. 39 pp.

Bischoff, J. L., Menking, K. M., Fitts, J. P., and Fitzpatrick, J. A., 1997. Climatic oscillations 10,000-155,000 yr B.P. at Owens Lake California reflected in glacial rock flour abundance and lake salinity in core OL-92. *Quaternary Research*, v. 48, no. 3: 313-325.

Burbank, D. W., 1981. A chronology of late Holocene glacier fluctuations on Mount Rainier, Washington. *Artic and Alpine Research*, vol. 13: 369-386.

Burrows, R. A., 2000. Glacial chronology and paleoclimatic significance of cirque moraines near Mts. Baker and Shuksan, North Cascade Range, Washington. MS thesis, Western Washington University. 92 pp.

Clark, D. H., 2003. Complex timing and patterns of glaciation in the American Cordillera during Termination 1. *Congress of the International Union for Quaternary Research*, v. 16: 231.

Clark, D. H., and Gillespie, A. R., 1997. Timing and significance of late-glacial and Holocene cirque glaciation in the Sierra Nevada, California. *Quaternary International*, v. 38/39: 21-38.

Clark, D. H., Bierman, P. R., and Larsen, P., 1995. Improving in situ cosmogenic chronometers. *Quaternary Research*, v.44, no. 3: 367-377.

Davis, P. T., 2003. Abrupt Late Pleistocene climatic reversals in Colorado and Wyoming: Evidence from lake sediments and moraines in cirques. *Abstracts with Programs- Geological Society of America*, v. 35, no. 6: 350.

Davis, P. T., 1994. Late-glacial moraines in American Cordillera of Younger Dryas Age?. *Abstracts with Programs- Geological Society of America*, v. 26, no. 7: 510.

Denton, G. H. and Porter, S. C., 1970. Neoglaciation: Mountain glaciers all over the world advanced several times since the end of the last major "ice age." Their fluctuations are a generalized record of global climatic changes over 6,000 years. *Scientific American*, v. 222, no. 6: 100-111.

Easterbrook, D. J., 2003. Cordilleran ice sheet glaciation of the Puget Lowland and Columbia Plateau and alpine glaciation of the North Cascade Range, Washington. *In* Swanson, T. W., ed., Western Cordillera and adjacent areas: Boulder, Colorado, *Geological Society of America Field Guide*, v. 4: 137-157.

Erikson, E. H. Jr., 1977. Petrology and petrogenesis of the Mount Stuart Batholith – plutonic equivalent of the high-alumina basalt association? *Contributions to Mineralogy and Petrology*, v. 60, 183-207.

Furbish, D. J. and Andrews, J. T., 1984. The use of hypsometry to indicate long-term stability and response of valley glaciers to changes in mass transfer. *Journal of Glaciology*, v. 30, no. 105: 199-211.

Grove, J. M., 1988. *The Little Ice Age*. London: Methuen. 498 pp.

Hagstrum, J. T. and Champion, D. E., 2002. A Holocene paleosecular variation record from ^{14}C-dated volcanic rocks in western North America. *Journal of Geophysical Research*, v. 107, no. B1: 8-1 – 8-14.

Hanna, R. L. and Verosub, K. L., 1988. A 3500-year paleomagnetic record of late Holocene secular variation from Blue Lake, Idaho. *Geophysical Research Letters*, v. 15, no. 7: 685-688.

Heikkinen, O., 1984. Dendrochronological evidence of variations of Colman Glacier, Mount Baker, WA, USA. *Artic and Alpine Research*, vol. 16: 53-64.

Heine, J. T., 1998. Extent, timing and climatic implications of glacier advances Mount Rainer, Washington, USA, at the Pleistocene/Holocene transition. *Quaternary Science Reviews*, v. 17: 1139-1148.

Heiri, O., Lotter, A. F., and Lemcke, G., 2001. Loss on ignition as a method for estimating organic and carbonate content in sediments: reproducibility and comparability of results. *Journal of Paleolimnology*, v. 25: 101-110.

Housen, B. A., Beck, Jr., M. E., Burmester, R. F., Fawcett, T., Petro, G., Sargent, R., Addis, K., Curtis, K., Ladd, J., Liner, N., Molitor, B., Montgomery, T., Mynatt, I., Palmer, B., Tucker, D., and White, I., 2003. Paleomagnetism of the Mount Stuart batholith Revisited Again: What has been learned since 1972? *American Journal of Science*, v. 303: 263-299.

Jackson, M., Gruber, W., Marvin, J., and Banerjee, S. K., 1988. Partial anhysteretic remanence and its anisotropy: Applications and grainsize-dependence. *Geophysical Research Letters*, v. 15, no. 5: 440-443.

Jelinek, V., 1981. Characterization of the magnetic fabric of rocks. *Tectonophysics*, v. 79: 63-67.

King, J. W. and Channell, J. E. T., 1991. Sedimentary magnetism, environmental magnetism, and magnetostratigraphy. *Reviews of Geophysics*, supplement, April, 1991, US National Report to IUGG: 358-370.

Kirschvink, J. L., 1980. The least-squares line and plane and the analysis of paleomagnetic data. *Geophysical Journal of the Royal Astronomical Society*, v.62, no. 3: 699-718.

Kovanen, D. J. and Easterbrook, D. J., 2001. Late Pleistocene, post-Vashon, alpine glaciation of the Nooksack drainage, North Cascades, Washington. *Geological Society of America Bulletin*, v. 113, no. 2: 274-288.

Kovanen, D. J. and Slaymaker, O., 2004. Deming Glacier fluctuations and theoretical equilibrium-line altitudes during the late Pleistocene and early Holocene Mount Baker, Washington, U.S.A.. *in review.*: 50pp

Leonard, E. M., 1974. Price Lake moraines: Neoglacial chronology and lichenometry study. MS thesis, Simon Fraser University. 102 pp.

Leonard, E. M., 1986a. Varve studies at Hector Lake, Alberta, Canada and the relationship between glacial activity and sedimentation. *Quaternary Research*, v. 25: 199-214.

Leonard, E. M., 1986b. Use of lacustrine sedimentary sequences as indicators of Holocene glacial history, Banff National Park, Alberta, Canada. *Quaternary Research*, v. 26: 218-231.

Leonard, E. M., 1989. Climatic change in the Colorado Rocky Mountains: Estimates based on modern climate at late Pleistocene equilibrium lines. *Arctic and Alpine Research*, v. 21, no. 3: 245-255.

Lund, S. P. and Banerjee, S. K., 1985. Late Quaternary paleomagnetic field secular variation from two Minnesota lakes. *Journal of Geophysical Research*, v. 90, no. 1: 803-825.

Mathewes, R. W., Heusser, L. E., and Patterson, R. T., 1993. Evidence for a Younger Dryas-like cooling event on the British Columbia coast. *Geology*, v. 21: 101-104.

Matthews, J. A. and Karlen, W., 1992. Asynchronous neoglaciation and Holocene climatic change reconstructed from Norwegian glaciolacustrine sedimentary sequences. *Geology*, v.20, no. 11: 991-994.

Meierding, T. C., 1982. Late Pleistocene glacial equilibrium-line altitudes in the Colorado Front Range: A comparison of methods. *Quaternary Research*, v. 18: 289-310.

Miller, C. D., 1969. Chronology of Neoglacial moraines in the Dome Peak area, North Cascade Range, Washington. *Artic and Alpine Research*, vol. 1: 49-66.

Mullineaux, D. R., 1986. Summary of pre-1980 tephra-fall deposits erupted from Mount St. Helens, Washington State, USA. *Bulletin of Vocanology*, v. 48: 17-26.

Osborn, G. and Luckman, B. H., 1988. Holocene glacier fluctuations in the Canadian Cordillera (Alberta and British Columbia). *Quaternary Science Reviews*, vol. 7: 115-128.

Paillard, D., Labeyrie, L., and Yiou, P., 1996. Macintosh program performs time-series analysis. *Eos Trans. AGU*, v.77: 379.

Porter, S. C., 1981. Glaciological evidence of Holocene climatic change. *in* Wigley, T. M. L., Ingram, M. L., and Farmer, G., (eds), *Climate and history: Studies in past climates and their impact on Man: Conference held at the University of East Anglia*, Cambridge: Cambridge Univ. Press. 82-110.

Porter, S. C., 1975. Equilibrium-line altitudes of late Quaternary glaciers in the Southern Alps, New Zealand. *Quaternary Research*, v. 5: 27-47.

Reasoner, M. A., 1993. Equipment and procedure improvements for a lightweight, inexpensive, percussion core sampling system. *Journal of Paleolimnology*, v. 8, no. 3: 273-281.

Ridge, J. C., Brennan, W. J., and Muller, E. H., 1990. The use of paleomagnetic declination to test correlations of late Wisconsinan glaciolacustrine sediments in central New York. *Geological Society of America Bulletin*, v. 102, no. 1: 26-44.

Rosenbaum, J. G., Reynolds, R. L., Smoot, J. P., Joseph, P., and Meyer, R., 2000. Anisotropy of magnetic susceptibility as a tool for recognizing core deformation; reevaluation of the paleomagnetic record of Pleistocene sediments from drill hole OL-92, Owens Lake, California. *Earth and Planetary Science Letters*, v. 178, no. 3-4: 415-424.

Schwehr, K. and Tauxe, L., 2003. Characterization of soft-sediment deformation: Detection of cryptoslumps using magnetic methods. *Geology*, v. 31, no. 3: 203-206.

Sigafoos, R. S. and Hendricks, E. L., 1961. Botanical evidence of the modern history of Nisqually Glacier, Washington. *U. S. Geological Survey Professional Paper, 387-A*. 20pp.

Sutherland, D. G., 1984. Modern glacier characteristics as a basis for inferring former climates with particular reference to the Loch Lomond Stadial. *Quaternary Science Reviews*, v. 3: 291-309.

Swanson, T. W. and Porter, S. C., 1997. New cosmogenic isotope ages for the last glaciation in the eastern North Cascade Range. *Abstracts with Programs- Geological Society of America*, v. 29, no. 6: 108.

Tabor, R. W., Waitt, Jr., R. B., Frizzell, Jr., V. A., Swanson, D. A., Byerly, G. R., and Bentley, R. D., 1982. Geologic map of the Wenatchee 1:100,000 Quadrangle, Central Washington. *United States Geological Survey*, Map 1-1311.

Thomas, P. A., 1997: Late Quaternary glaciation and volcanism on the south flank of Mt. Baker, Washington. MS thesis, Western Washington University. 98 pp.

Thomas, P. A., Easterbrook, D. J., and Clark, P. U., 2000. Early Holocene glaciation on Mount Baker, Washington State, USA. *Quaternary Science Reviews*, v. 19: 1043-1046.

Torsnes, I., Rye, N. and Nesje, A., 1993. Modern and Little Ice Age equilibrium-line altitudes on outlet valley glaciers from Jostedalsbreen, Western Norway: an evaluation of different approaches to the calculation. *Artic and Alpine Research*, v. 25, no. 2: 106-116.

Verosub, K. L., Mehringer, Jr., P. J., and Waterstraat, P., 1986. Holocene secular variation in Western North America: Paleomagnetic record from Fish Lake, Harney County, Oregon. *Journal of Geophysical Research*, v. 91, no. B3: 3609-3623.

Waitt, Jr., R. B., Yount, J. C., and Davis, P. T., 1982. Regional significance of an early Holocene moraine in Enchantment Lakes Basin, North Cascade Range, Washington. *Quaternary Research*, v. 17: 191-210.

Watkins, S. J. and Maher, B. A., 2003. Magnetic characterisation of present-day deep-sea sediments and sources in the North Atlantic. *Earth and Planetary Science Letters*, v. 214: 379-394.

Yamaguchi, D. K., 1983. New tree-ring dates for recent eruptions of Mount St. Helens. *Quaternary Research*, v. 20, no. 2: 246-250.

Zdanowicz, C. M., Zielinski, G. A., and Germani, M. S., 1999. Mount Mazama eruption: Calendrical age verified and atmospheric impact assessed. *Geology*, v.27, no. 7: 621-624.

Zielinski, G. A. and Davis, P. T., 1987. Late Pleistocene Age of the type Temple Lake Moraine, Wind River Range, Wyoming, U.S.A. *Geographie physique et Quaternair*, v. 41: 397-401.

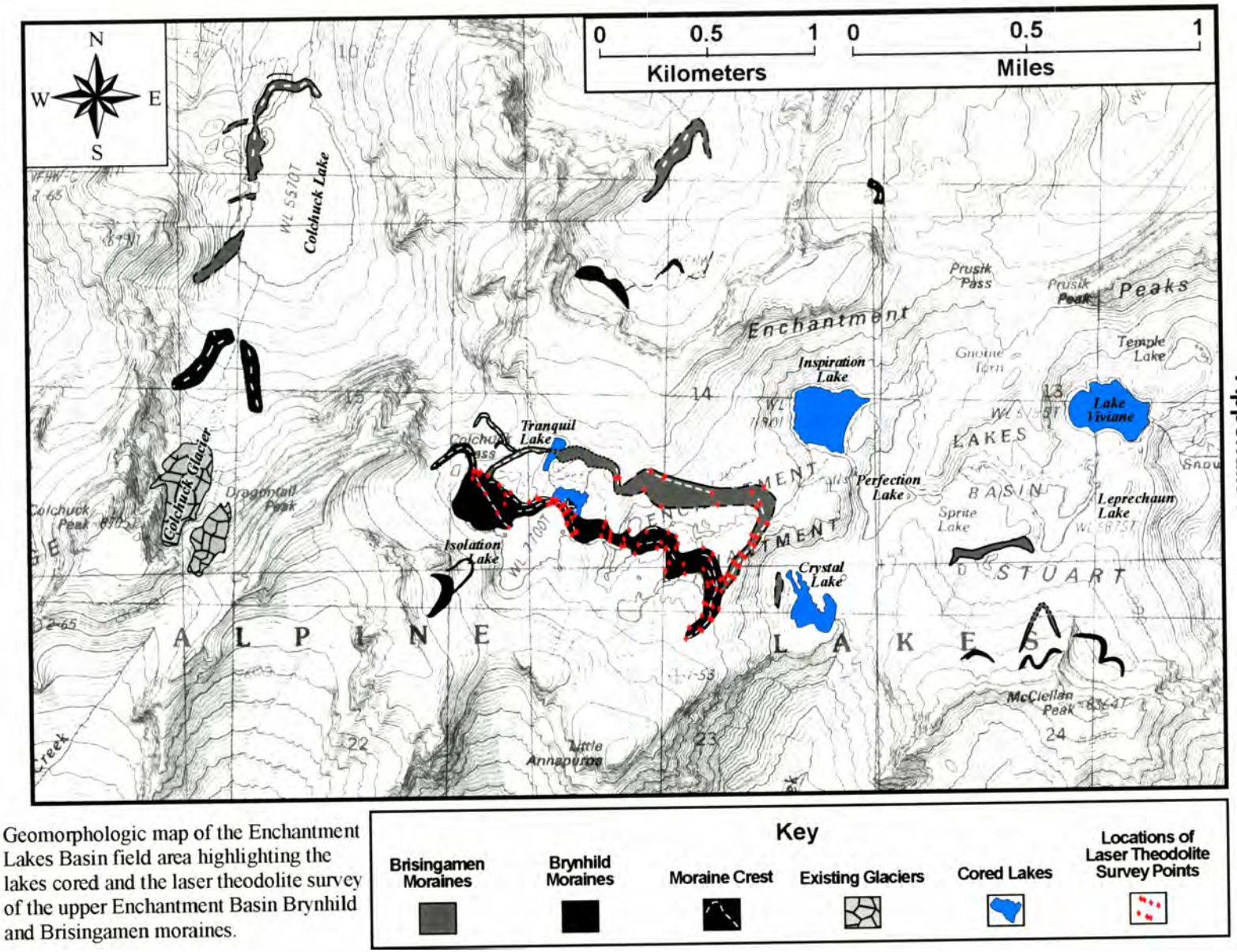

Appendix 1. Geomorphologic map of the Enchantment Lakes Basin field area highlighting the lakes cored and the laser theodolite survey of the upper Enchantment Basin Brynhild and Brisingamen moraines.

Appendix 2. Table of Paleomagnetic data for Lake Viviane Core 1, including NRM moment and the results of the principle component analysis.

Depth (cm)	Sample Name	NRM Moment (10E-8 Am^2)	Declination	Inclination	Step of start (mT)	Step of end (mT)	Number of points	MAD	Angle to Origin
1	LV C1 0-2	1.2226	275.4	71.3	5	35	11	27.3	5.9
5	LV C1 4-6	15.427	169.8	41.6	17.5	45	8	11.7	3.8
9	LV C1 8-10	27.443	180.9	28	12.5	25	5	4.4	2.4
11.5	LV C1 10.5-12.5	22.49	121.3	58.2	7.5	50	13	12.8	5.6
15	LV C1 14-16	1.579	124.3	69	12.5	50	11	18.3	10.6
17	LV C1 16-18	1.6956	116	69.7	5	50	14	8.8	3.1
19	LV C1 18-20	1.222	197.4	74.8	5	40	12	16.1	14.1
23	LV C1 22-24	2.5367	81.2	67.2	12.5	65	14	16.8	5.1
27	LV C1 26-28	4.2651	58.7	66.3	10	85	17	9	3
31	LV C1 30-32	6.6763	41.9	74.5	12.5	40	9	9.7	8.5
35	LV C1 34-36	8.8626	65.8	68.9	12.5	85	16	6.8	1.7
39	LV C1 38-40	5.5346	48.5	64.2	10	70	15	6.4	1.6
41	LV C1 40-42	2.3555	71.4	58.1	10	85	15	9.8	1.3
43	LV C1 42-44	3.0021	56.1	65	12.5	80	15	15.5	5.7
48	LV C1 47-49	194.28	38	61.1	7.5	140	20	1.3	0.2
51	LV C1 50-52	13.574	63.2	69.4	12.5	70	14	8.5	3.5
55	LV C1 54-56	19.408	58.6	70.3	10	90	17	2.6	0.7
59	LV C1 58-60	6.6406	66.3	73	10	70	14	3.6	1.4
63	LV C1 62-64	4.8882	78.7	81.3	12.5	80	14	8.5	3.4
67	LV C1 66-68	7.5043	45.7	72.6	5	85	18	8.7	2.9
71	LV C1 70-72	4.6082	69	72.4	15	95	15	4.9	3.4
75	LV C1 74-76	4.5082	70.9	63.3	7.5	85	18	10.2	1.2

Appendix 3. Table of the results of the AMS-radiocarbon analyses. All samples were analyzed at the Center for Accelerator Mass Spectrometry (CAMS), Lawrence Livermore National Laboratory. ^{14}C ages were calibrated using the University of Washington Quaternary Isotope Lab Radiocarbon Calibration Program Rev. 4.3.

Sample Name	CAMS Sample #	Lake Core	Depth in Core (cm)	Material	^{14}C Age	±	cal. yr B.P.	2 sigma age range
CC1Tp-216.5	73431	Crystal Lake Core 1	16.5	wood	560	40	547	648-514
CC1Tp-425	73432	Crystal Lake Core 1	25	wood	1630	50	1529	1689-1409
CC1Bt-S203 .04mgC	73426	Crystal Lake Core 1	84.3	wood	3840	150	4240	4806-3783
CC1Bt-S59.9	73427	Crystal Lake Core 1	90.8	wood	4150	40	4694	4830-4528
CC1Bt-S732	73428	Crystal Lake Core 1	113.3	wood	5170	60	5922	6168-5751
CC1Bt-S939 .1mgC	73429	Crystal Lake Core 1	120.3	wood	5360	70	6127	6293-5940
CC1Bt-S1359	73430	Crystal Lake Core 1	140.3	wood	6180	70	7088	7253-6809
CC1Bt-S1883 .05 mgC	73435	Crystal Lake Core 1	164.3	wood	6660	140	7530	7786-7273
ELB-1	79723	Lake Viviane Core 5	171.2	wood fibers	6800	120	7627	7922-7432
ELB-2-1	79724	Lake Viviane Core 5	209.2	leaf part	8210	40	9204	9397-9027
ELB-2-2 .05mgC	79830	Lake Viviane Core 5	209.2	lichen	8580	180	9540	10155-9134
ELB-3	80680	Lake Viviane Core 5	209.2	bulk sediment	8480	40	9512	9534-9431
ELB-4	80681	Lake Viviane Core 5	78.75	bulk sediment	9715	40	11168	11199-10890

Appendix 4

Age-depth analysis using AnalySeries

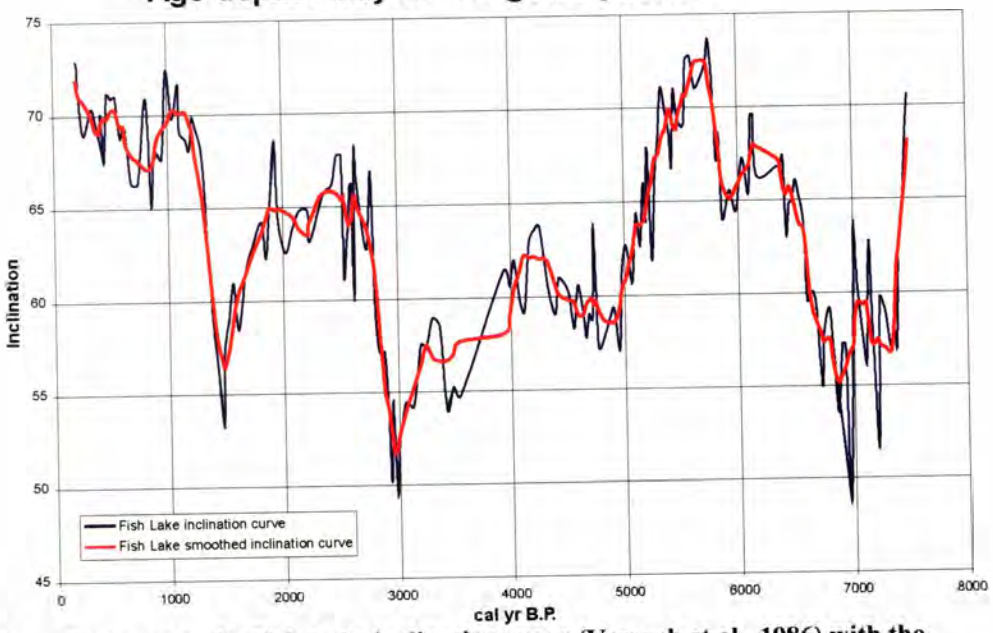

Figure 1. To compare the Fish Lake inclination curve (Verosub et al., 1986) with the volcanic rock (Hagstrum and Champion, 2002) and Lake Viviane inclination curves, the Fish Lake curve was first smoothed to eliminate the high frequency signal. The Fish Lake inclination curve was smoothed using an 11-point least squares smoothing function.

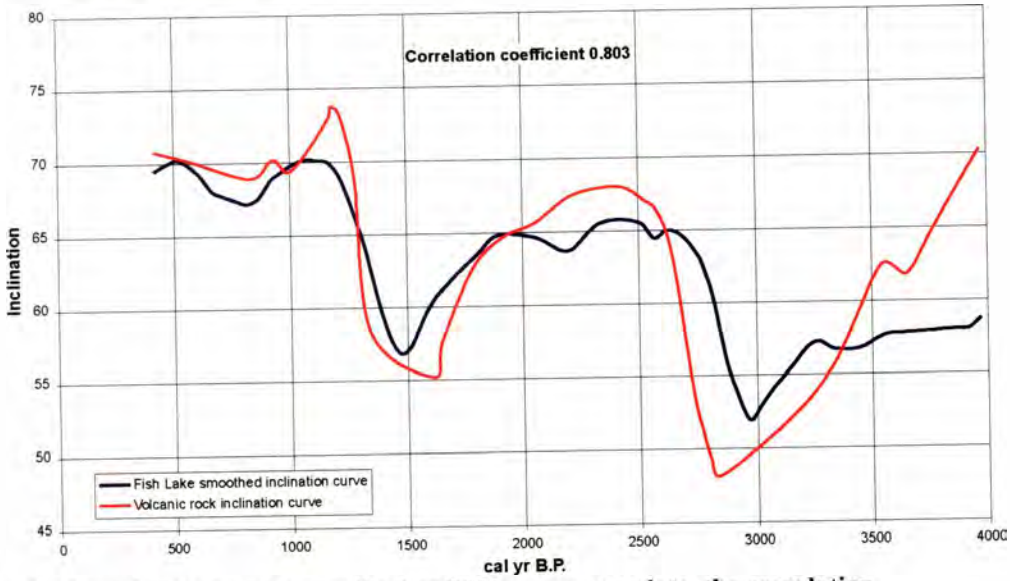

Figure 2. In order to show how well other PSV curves correlate, the correlation coefficient between the Fish Lake inclination curve (Verosub et al., 1986) and volcanic rock inclination curve (Hagstrum and Champion, 2002) was calculated. To get the best correlation, the 280 year offset between the two curves (Hagstrum and Champion, 2002) was eliminated by shifting the volcanic rock inclination curve back in time 280 years.

Appendix 4

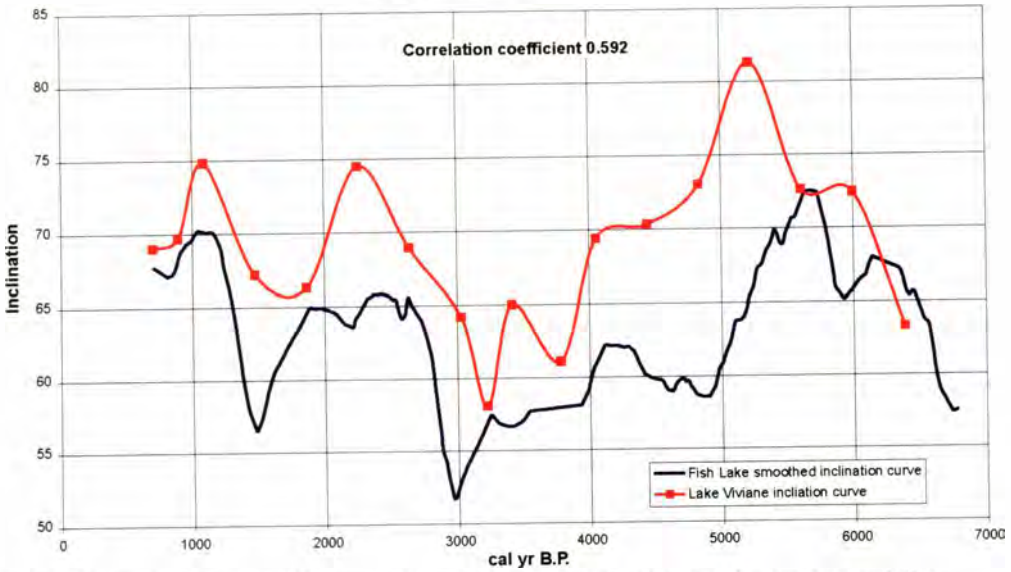

Figure 3. The correlation coefficient between the Fish Lake inclination curve and the sedimentation rate based Lake Viviane inclination curve age model. The sedimentation rate age model for the Lake Viviane inclination curve is based on a constant sedimentation rate between the The Mt. St Helens Wn tephra (475 cal. yr B.P) and the Mt. St Helens Yn tephra (3780 cal. yr B.P.). This sedimentation rate (97 yr/cm) was then applied to the pre Mt. St Helens Yn tephra sediment.

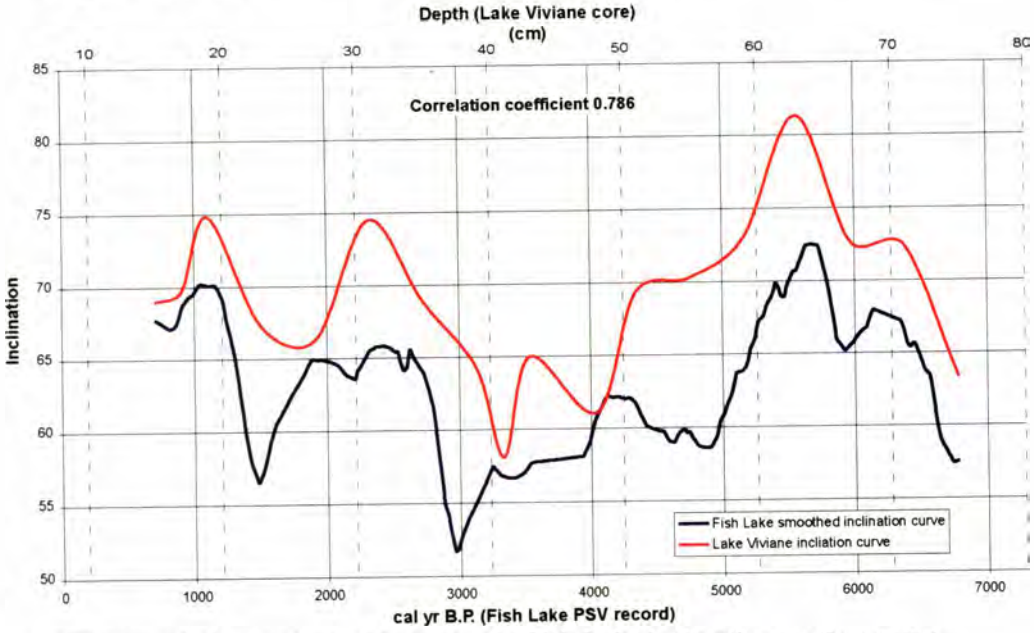

Figure 4. The correlation coefficient between the Fish Lake inclination vs. time curve and the Lake Viviane inclination vs. depth curve. This graph represents the first step in transforming the Lake Viviane inclination versus depth curve into an inclination versus age curve using the Fish Lake inclination curve as the reference signal.

Appendix 4

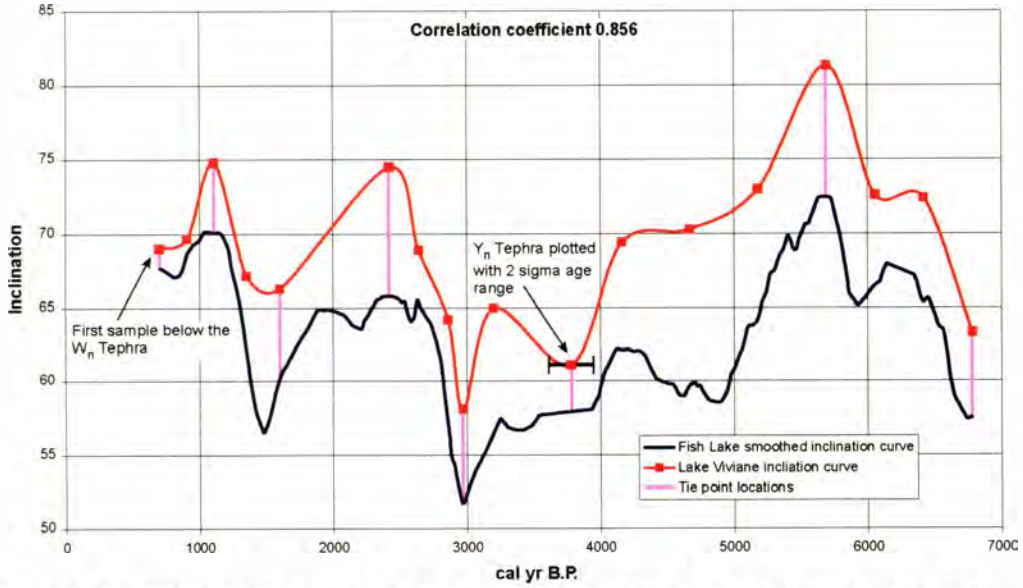

Figure 5. The result of adjusting the Lake Viviane inclination vs. depth curve to the Fish Lake inclination vs. time curve using the tie points shown and assuming a constant sedimentation rate between tie points.

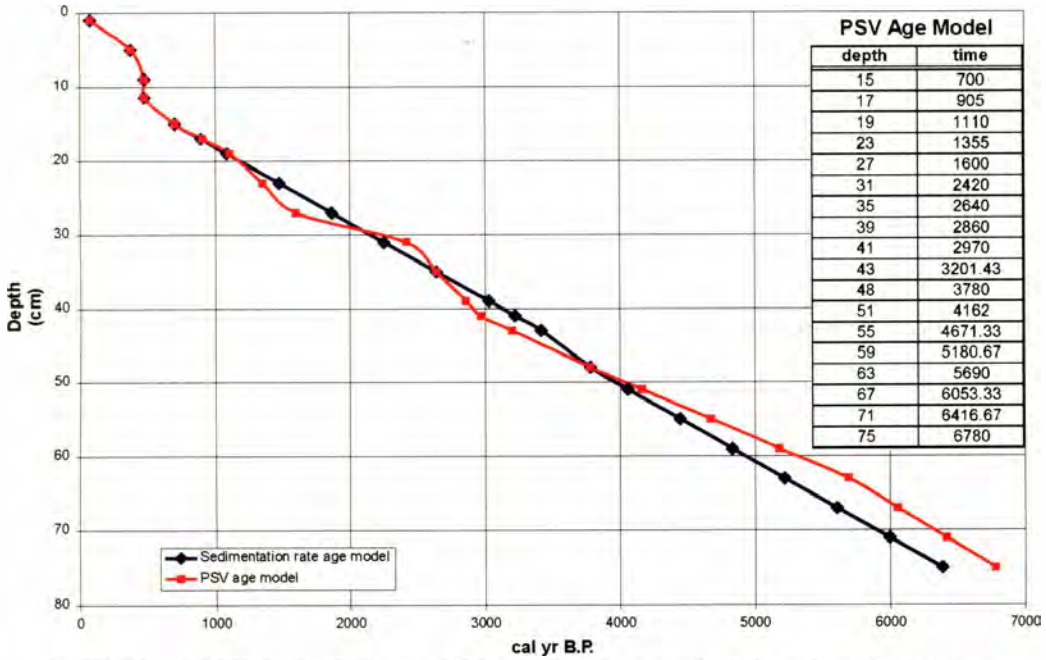

PSV Age Model

depth	time
15	700
17	905
19	1110
23	1355
27	1600
31	2420
35	2640
39	2860
41	2970
43	3201.43
48	3780
51	4162
55	4671.33
59	5180.67
63	5690
67	6053.33
71	6416.67
75	6780

Figure 6. The final PSV derived age model for Lake Viviane plotted against the intra-tephra sedimentation rate derived age model for Lake Viviane.